12 years of continuous atmospheric O_2, CO_2 and APO data from Weybourne Atmospheric Observatory in the United Kingdom

Karina E. Adcock[1], **Penelope A. Pickers**[1], **Andrew C. Manning**[1], **Grant L. Forster**[1,2],
Leigh S. Fleming[1,a], **Thomas Barningham**[3], **Philip A. Wilson**[1], **Elena A. Kozlova**[4], **Marica Hewitt**[1],
Alex J. Etchells[5], **and Andy J. Macdonald**[1]

[1]Centre for Ocean and Atmospheric Sciences, School of Environmental Sciences,
University of East Anglia, Norwich, United Kingdom
[2]National Centre for Atmospheric Science, University of East Anglia, Norwich, United Kingdom
[3]British Antarctic Survey, Natural Environment Research Council, Cambridge, United Kingdom
[4]Faculty of Environment, Science and Economy, University of Exeter, Exeter, United Kingdom
[5]Research and Specialist Computing, University of East Anglia, Norwich, United Kingdom
[a]now at: GNS Science, Gracefield, Lower Hutt, 5040, New Zealand

Correspondence: Karina E. Adcock (karina.adcock@uea.ac.uk)

Abstract. We present a 12-year time series of continuous atmospheric measurements of O_2 and CO_2 at the Weybourne Atmospheric Observatory in the United Kingdom. These measurements are combined into the term atmospheric potential oxygen (APO), a tracer that is invariant to terrestrial biosphere fluxes. The CO_2, O_2 and APO datasets discussed are hourly averages between May 2010 and December 2021. We include details of our measurement system and calibration procedures, and describe the main long-term and seasonal features of the time series. The 2 min repeatability of the measurement system is approximately ± 3 per meg for O_2 and approximately ± 0.005 ppm for CO_2. The time series shows average long-term trends of 2.40 ppm yr^{-1} (2.38 to 2.42) for CO_2, -24.0 per meg yr^{-1} for O_2 (-24.3 to -23.8) and -11.4 per meg yr^{-1} (-11.7 to -11.3) for APO, over the 12-year period. The average seasonal cycle peak-to-peak amplitudes are 16 ppm for CO_2, 134 per meg for O_2 and 68 per meg for APO. The diurnal cycles of CO_2 and O_2 vary considerably between seasons. The datasets are publicly available at https://doi.org/10.18160/Z0GF-MCWH (Adcock et al., 2023) and have many current and potential scientific applications in constraining carbon cycle processes, such as investigating air–sea exchange of CO_2 and O_2 and top-down quantification of fossil fuel CO_2.

1 Introduction

Carbon dioxide (CO_2) and oxygen (O_2) vary in the atmosphere due to a range of processes including terrestrial biosphere exchange, combustion (e.g. fossil fuels and wild fires) and air–sea gas exchange with the oceans. Terrestrial biosphere fluxes of O_2 and CO_2 are strongly anti-correlated, with a stoichiometric exchange ratio of 1.05–1.10 moles of O_2 consumed per mole of CO_2 produced (or vice versa) (Severinghaus, 1995; Keeling and Manning, 2014). In fos-

sil fuel combustion O_2 is consumed, and CO_2 is produced, with a globally weighted average stoichiometric exchange ratio of about 1.38 mol mol^{-1} (Keeling and Manning, 2014). There is no fixed stoichiometric coupling between CO_2 and O_2 in ocean–atmosphere fluxes due to their different seawater chemistry properties (Keeling et al., 1993). Due to these varied relationships between CO_2 and O_2, measuring atmospheric O_2 concurrently to CO_2 provides a wealth of additional information on carbon biogeochemical cycles than can be achieved by measuring CO_2 alone.

Making high-precision measurements of O_2 mole fractions in the atmosphere is technically challenging as variations in O_2 are relatively very small compared to the atmospheric background (variations of the order of 10 ppm against a background of $\sim 210\,000$ ppm). As such, atmospheric O_2 mole fractions are typically reported as changes in the ratio of O_2 to N_2, relative to a reference O_2/N_2 ratio (Keeling and Shertz, 1992).

$$\delta(O_2/N_2) = \frac{(O_2/N_2)_{sample} - (O_2/N_2)_{reference}}{(O_2/N_2)_{reference}}. \qquad (1)$$

This study uses a O_2/N_2 reference derived from a suite of compressed air reference gases stored in high-pressure tanks and maintained by the Scripps Institution of Oceanography, USA (SIO; Sect. 2.2; Keeling et al., 2007). Given that variations of $\delta(O_2/N_2)$ are small, the values are multiplied by 10^6 and expressed in "per meg" units (Keeling and Shertz, 1992). Since mole fractions are relative to the total amount of air, changing the total number of molecules, for example by changing the number of CO_2 molecules, will make it appear as if the amounts of O_2 and N_2 are changing even when they are not. This dilution effect is problematic for O_2 and N_2 because they are not trace gases; however, reporting O_2 as the O_2/N_2 ratio circumvents this issue. The dilution effect also exists for trace gases but has a negligible effect. Natural variations in N_2 are much smaller than O_2 (Manning and Keeling, 2006), and, therefore, any changes in the O_2/N_2 ratio can be assumed to be due to a change in O_2. When measuring O_2, CO_2 must also be measured concurrently, and a correction applied to account for changes in CO_2. For simplicity, in this paper, we refer to O_2 variations as O_2 mole fraction changes.

Atmospheric potential oxygen (APO) is a calculated term that is helpful to further investigate some of the processes that affect both O_2 and CO_2, for example ocean processes (e.g. Ishidoya et al., 2022; Tohjima et al., 2015; Resplandy et al., 2019; Nevison et al., 2020; Pickers et al., 2017) and fossil fuel combustion (Pickers, 2016; Chevallier and the WP4 CHE partners, 2021; Pickers et al., 2022). APO is the sum of atmospheric O_2 and atmospheric CO_2 multiplied by the $O_2 : CO_2$ molar exchange ratio of terrestrial biosphere–atmosphere exchange (Stephens et al., 1998). APO is thus invariant to terrestrial biosphere processes and is influenced by most fossil fuel emissions, due to their different exchange ratios, and by air–sea gas exchange of O_2 and CO_2. APO is calculated according to:

$$APO = O_2 + \frac{\alpha_L \times (CO_2 - 350)}{S_{O_2}}, \qquad (2)$$

where α_L is the global average terrestrial biosphere exchange ratio, 1.10 mol mol^{-1} (Severinghaus, 1995), S_{O_2} is the standard atmospheric mole fraction of O_2, 0.2095 (Machta and Hughes, 1970), and 350 is an arbitrary reference value used to express APO on the Scripps Institution of Oceanography

(SIO) APO scale. CO_2 is the measured CO_2 mole fraction, expressed in parts per million (ppm), and O_2 is the measured O_2 reported as $\delta(O_2/N_2)$ ratio changes. Both APO and O_2 are expressed in per meg units.

We present continuous in situ measurements of atmospheric O_2 and CO_2 mole fractions from Weybourne Atmospheric Observatory (WAO). WAO is a field station located on the north Norfolk coast in a rural part of the United Kingdom ($52.95°$ N, $1.12°$ E, Fig. 1). The station was established in 1992 by the University of East Anglia (UEA) and is a United Nations World Meteorological Organization Global Atmosphere Watch (WMO/GAW) "Regional" station, a UK National Centre for Atmospheric Science Atmospheric Measurement and Observation Facility (NCAS/AMOF), and a European Integrated Carbon Observation System (ICOS) "Class II" station. The O_2 and CO_2 measurement system is housed in an air-conditioned concrete building. The sample inlets sit atop a 10 m mast, ~ 27 m above sea level and ~ 50 m inland from the North Sea coastline. In addition to continuous measurements of atmospheric O_2 and CO_2, other species routinely measured include CO, CH_4, H_2, O_3, N_2O, SF_6, ^{222}Rn, NO, NO_2, $PM_{2.5}$, PM_{10}, SO_2, NH_3, $\delta^{13}C$-CO_2, $\delta^{18}O$-CO_2, and $\delta^{17}O$-CO_2, as well as basic meteorological parameters (http://www.weybourne.uea.ac.uk, last access: 17 November 2023).

In the remainder of this paper, Sect. 2 describes the measurement system and the seasonal decomposition methodologies, and Sect. 3 provides an assessment of the measurement system's performance via intercomparison programme results, and repeatability and compatibility measures. In Sect. 4, we present the main features of the dataset: long-term trends, seasonal cycles, and diurnal cycles of CO_2, O_2 and APO. This analysis builds on work previously presented in the PhD theses of Wilson (2012) and Barningham (2018).

2 Methods

2.1 Analytical setup

The CO_2 and O_2 measurement system used at WAO is similar to those described in Stephens et al. (2007), Thompson et al. (2007) and Pickers et al. (2017). The WAO measurement system was first described in Patecki and Manning (2007) before it was deployed at WAO; it was also described in Pickers et al. (2022) and in the PhD theses of Wilson (2012) and Barningham (2018). There have been many modifications and upgrades to the system since it was first installed. The following description and Fig. 2 present the system as it stands in 2023.

There are two inlet lines, and the measurement system alternates sampling air between these two inlet lines every 2 h to diagnose for leaks, blockages, or other faults. The inlet lines are approximately 14 m long and are made of Synflex type 1300 tubing with an outer diameter of $1/4''$.
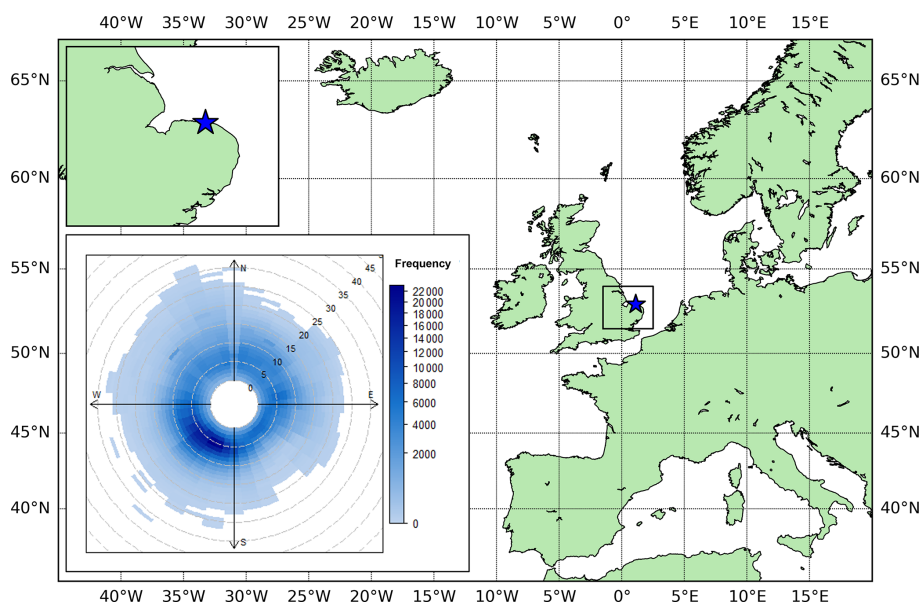
Figure 1. Map showing the location of the Weybourne Atmospheric Observatory (WAO, 52.95° N, 1.12° E) as a blue star. Bottom left inset: polar frequency plot showing wind speed ($m\,s^{-1}$) and wind direction at WAO averaged over the period 2016–2021. The frequency is the number of points with that wind speed and wind direction.

Each inlet line includes an aspirated air inlet (Aspirated Radiation Shield Model No. 43502, Read Scientific Ltd.), whereby the inlet samples from a moving airstream and shields the entrance from solar radiation, to avoid fractionation of O_2 molecules relative to N_2 (Blaine et al., 2006) and a small diaphragm pump (KNF Neuberger Inc.; model PM27653-N86ATE) to draw air through the inlet tubing at $100\,mL\,min^{-1}$.

Air from the inlets passes through a two-stage drying system to dry the sample air to $< 1\,ppm$ water vapour, which prevents dilution effects caused by water vapour that would otherwise bias the O_2 measurements (Stephens et al., 2007). The first stage of the drying system is a Peltier element thermo-electric cooler (Tropicool, model XC3000A), set at approximately $1\,°C$. Water condenses out of the air and is drained away by peristaltic pumps (Cole Parmer, Masterflex). The Tropicool consists of stainless-steel traps filled with 4 mm diameter Pyrex glass beads (to provide greater surface area to promote water condensation). Traps are positioned both upstream and downstream of the diaphragm pump; the downstream pump provides better water condensation because of the above ambient pressure provided by the pump ($\sim 3\,bar$), whereas the upstream pump prevents water build up in the pump itself. The second stage of the drying system is a VT490D cryogenic cooler (SP Scientific), which contains traps filled with 4 mm diameter Pyrex glass beads in a 4 L ethanol bath, and achieves a dew point of approximately $-80\,°C$.

The CO_2 mole fraction is measured by a non-dispersive infrared (NDIR) CO_2 analyser from Siemens Corp., model Ultramat 6E and the O_2 mole fraction is measured by an "Oxzilla", a dual fuel cell O_2 analyser from Sable Systems International Inc. The fuel cells contain a gas-permeable membrane across which O_2 from the air permeates and undergoes electrochemical reduction in the cells, which contain a lead anode in an acidic electrolyte solution. The Ultramat and Oxzilla analysers are both differential analysers and are placed in series. Sample air flows through one side of the analysers, and air from the Working Tank (WT, see Sect. 2.2) flows continuously through the other side of the analysers; air from calibration, quality control and intercomparison cylinders passes through the "sample" side. The flow rate of the measurement system (both the sample and working reference sides) is set to $100\,mL\,min^{-1}$ using a mass flow controller (MFC, Fig. 2). The pressures and flow rates are carefully balanced to be the same on both the sample air and WT air sides of the analysers. This balance is achieved with a differential pressure transducer (MKS Instruments, model Baratron 223B), which measures the pressure difference between the sample and WT air streams and then adjusts the sample side pressure to match the pressure of the WT air using a fast-response solenoid valve (MKS Instruments Inc., 248A; Fig. 2).

A four-way switching solenoid valve (Numatics, model TM series) immediately upstream of the Oxzilla switches the sample air and WT air between each of the fuel cells every 60 s. Switching between sample air and WT air helps to eliminate short-term drift and increases the signal to noise ratio, since the amplitude of the fuel cell difference is doubled, but the noise remains the same (Stephens et al., 2007). The first 30 s of data after every switch are discarded. Using the remaining 30 s of data, the difference between the fuel cells is
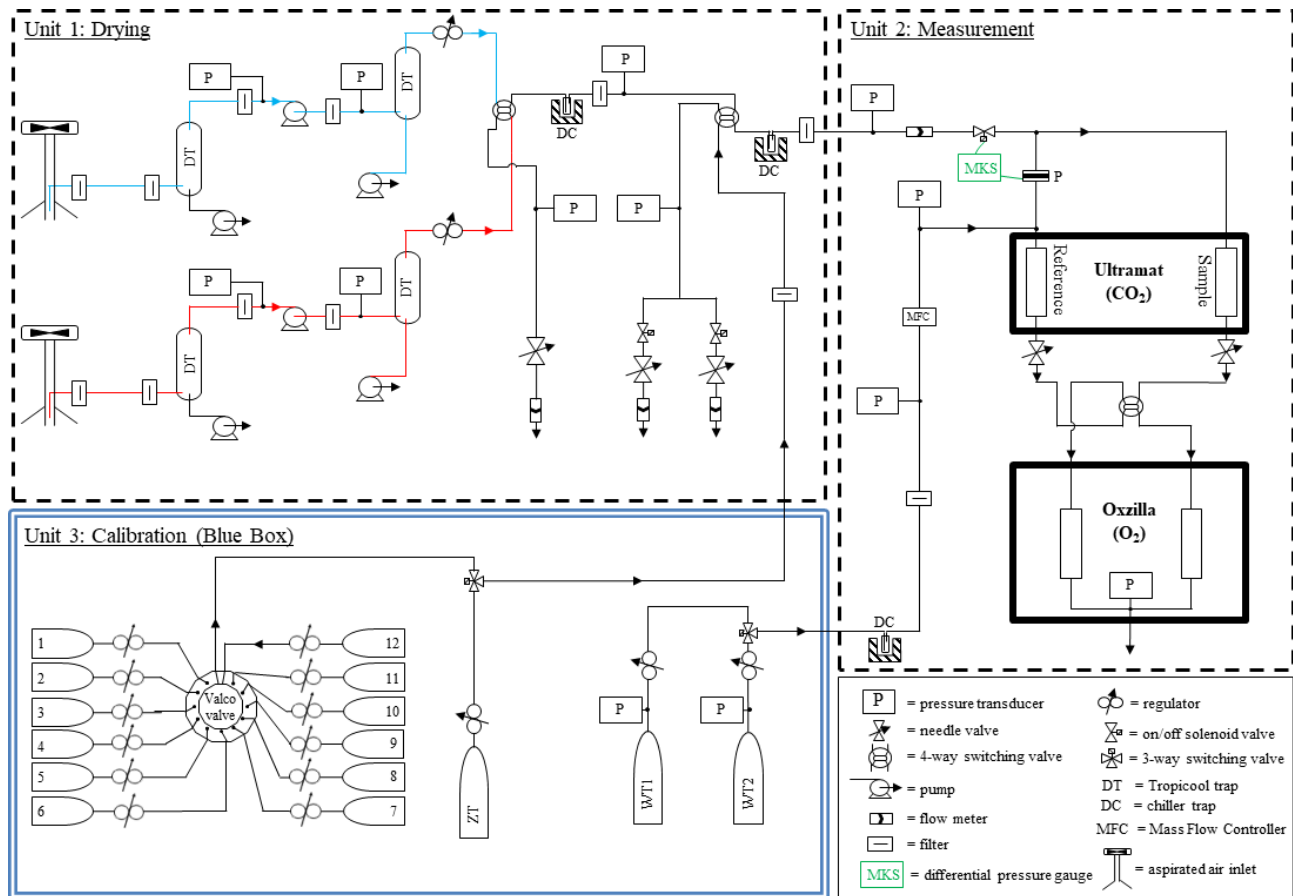
Figure 2. Gas handling diagram of the Weybourne Atmospheric Observatory (WAO) O$_2$ and CO$_2$ measurement system. The drying, measurement, and calibration units are shown in separate boxes. The "red" and "blue" inlet lines are coloured accordingly, and the green colouring denotes the "MKS" differential pressure gauge. The cylinders numbered 1–12 in the "Blue Box" demonstrate the maximum capacity of the multi-position "Valco" valve; these normally comprise of calibration cylinders, cylinders that are periodically measured as part of intercomparison programmes, Target Tanks (TTs), Zero Tanks (ZTs) and Working Tanks (WTs); see main text for details.

calculated. We refer to the fuel cell difference as the "double differential O$_2$ value", and it is effectively twice the O$_2$ mole fraction (Stephens et al., 2007). The measurement system reports an O$_2$ and CO$_2$ measurement every 2 min.

As shown in Fig. 2, the measurement system includes several pressure transducers, flow metres, solenoid valves, a flow controller, and temperature sensors (not shown in Fig. 2) that are all connected to an electronics control box (custom built in-house). Bespoke software (custom built in-house) enables the automation of many of the routine processes and minimises human intervention. The software's automation functionality includes: measuring cylinders at predetermined intervals; switching between the two inlet sample lines; flushing sample or cylinder air prior to analysis, processing analyser signals to calculate calibrated mole fractions in near real-time; rejecting calibrations outside a set range and notifying the user when key diagnostics stray outside of acceptable ranges. The software also records all of the analyser and diagnostic data (i.e. pressure, flow and temperature data) and

routinely backs up all data files. In addition, the system can be accessed and controlled remotely, with the software displaying most of the data in near real-time.

2.2 Calibration procedures

The measurement system includes a calibration unit, consisting of a thermally insulated housing for gas cylinder stabilisation, a so-called "Blue Box", where high-pressure cylinders are stored horizontally, a requirement for high-precision O$_2$ measurements (Keeling et al., 2007) that minimises thermal and gravitational fractionation of O$_2$ and N$_2$ molecules inside the cylinders. Our calibration procedures are similar to those detailed for O$_2$ and CO$_2$ in Kozlova and Manning (2009). Stored in the "Blue Box" are Working Tanks (WTs), Working Secondary Standards (WSSs), Zero Tanks (ZTs) and Target Tanks (TTs), and occasionally cylinders that are part of intercomparison programmes.

A cylinder containing dry, compressed air, known as a Working Tank (WT), is continuously run through the reference side of the differential Ultramat and Oxzilla analysers. CO_2 and O_2 are measured by comparing the CO_2 and O_2 in the air from the inlets (i.e. the sample side) to the CO_2 and O_2 in the air from the WT. By measuring the difference, any analyser response variability independent of the atmospheric mole fractions, for example from changes in room temperature or atmospheric pressure, is largely mitigated, since these changes will affect both the inlet air and WT air to roughly the same degree (Stephens et al., 2007).

A suite of three Working Secondary Standards (WSSs), which have high, medium, and low mole fractions of O_2 and CO_2 spanning the typical range of mole fractions observed at the station, is used to calibrate the analysers every 47 h (see calibration scale information below). The Ultramat exhibits a non-linear response to CO_2, so a quadratic equation ($y = ax^2 + bx + c$) is used in order to appropriately fit the analyser response function. The Oxzilla exhibits a linear response, so a linear equation is used ($y = bx + c$). With the exception of the CO_2 c-term, the calibration coefficients are redetermined every 47 h, and then these new values are used until the next calibration.

The CO_2 c-term (sometimes called the zero coefficient) is redetermined every 3 or 4 h using a Zero Tank (ZT), which is a cylinder filled with ambient air, and is run immediately after every calibration and then every 3 or 4 h afterwards. This CO_2 c-term adjustment is done to correct for baseline response drift in the Ultramat analyser, which is predominately due to room temperature fluctuations in-between calibrations. The ZT correction is only required for the CO_2 measurements, as the double differential switching accounts for analogous short-term temperature related drift in the O_2 analyser. A Target Tank (TT), also filled with ambient air, is typically measured every 11 h as a quality control check on both the measurement system and the calibration procedures.

All cylinders used are 40 or 50 L high-pressure aluminium cylinders (Luxfer Gas Cylinders Inc.) filled with very dry air (< 1 ppm water vapour content) to ~ 200 bar, at the Cylinder Filling Facility (CFF) at the UEA before being deployed at WAO. The O_2 and CO_2 mole fractions in the WSSs and the TT are pre-determined at UEA's Carbon Related Atmospheric Measurement (CRAM) Laboratory, by measuring the cylinders using a bespoke Vacuum Ultraviolet (VUV) absorption analyser (Stephens et al., 2003) for O_2 and a Siemens Ultramat 6F analyser for CO_2, against a suite of primary standards obtained from NOAA (National Oceanic and Atmospheric Administration), USA and Scripps Institution of Oceanography (SIO) (see calibration scale information below). The WSSs and TTs are used at WAO until the cylinder pressure is ~ 30 bar, and the WTs and ZTs are used until the cylinder pressure is ~ 5 bar, as there is frequently outgassing of gases from cylinder walls at low cylinder pressures.

From its inception to June 2014, the WAO CO_2 data were reported on the SIO CO_2 calibration scale. From July 2014 to December 2021 the CO_2 data were reported on the WMO CO_2 X2007 scale. Presently, all the data from October 2007 to December 2021 have been transferred onto the WMO CO_2 X2019 scale using Eq. (6) in Hall et al. (2021). The WMO CO_2 X2019 calibration scale is maintained by the Central Calibration Laboratory (CCL) at the NOAA Earth System Research Laboratories (ESRL) Global Monitoring Laboratory (GML). The O_2 measurements are reported on the SIO "S2" scale that was used by SIO from April 1995 to August 2017 (Keeling et al., 2020). For O_2 measurements there is no formally recognised scale but most laboratories within the global O_2 community use or are linked to the SIO scale.

The measurement system was first installed at WAO in October 2007; however, between October 2007 and May 2010, the system was still being developed and underwent major changes, leading to large gaps in the dataset and much of the data being of unknown quality and with calibration scale issues. Therefore the data from this period have been excluded, and only data from May 2010 to December 2021 are publicly available and are discussed in this paper.

2.3 Seasonal decomposition

The baselines of all three species were calculated from the hourly averages with the Robust Extraction of Baseline Signal (REBS) method using the RFBaseline function within the IDPMisc package in R (Ruckstuhl et al., 2012; 2020). The RFBaseline function has three adjustable parameters: span, bi-weight function (b), and the number of iterations (maxit). The span is the smoothing time period, based on the frequency of data points. We have used a value of 0.01, which applies a smoothing window with a period of approximately 4 weeks, which we think is the most appropriate for distinguishing regional and background variability. The bi-weight function uses asymmetrical weighting, which is appropriate for CO_2 and O_2, where short-term excursions from the baseline are mostly uni-directional (positive for CO_2; negative for O_2); here, we used 0.01, and the number of iterations used is (4,0).

The time series were decomposed using the REBS results and STL (Seasonal Trend decomposition using LOESS (locally weighted scatterplot smoothing); Cleveland et al., 1990), so that salient features in long-term trends and seasonality can be described and quantified. The STL function (in R) performs a moving average calculation to separate the trend, seasonal and random components of the time series. STL has two smoothing parameters: s.window, which is the number of years to use when estimating the seasonal component, and t.window, which is the number of consecutive observations to use when estimating the trend. We used an s.window of 5 years (this value is often used in other studies (Pickers and Manning, 2015)) and a t.window of 13 149. Cleveland et al. (1990) suggests that the t.window should be approximately 1.5 to 2 times the number of observations in each year, for hourly data, that is 8766 h per year

$(365.25 \cdot 24 = 8766)$, and $1.5 \cdot 8766 = 13\,149$. The decomposed time series are shown in the Supplement (Figs. S2–S4).

Since the currently available version of STL cannot handle gaps in the time series, the REBS results were interpolated using the na_seadec function in the imputeTS package in R (algorithm = "interpolation", option = "spline"), prior to decomposition using STL. Gap filling is to take account of times when sample air is not being measured because of routine cylinder analyses, because of scheduled system maintenance, or because of inadvertent downtimes owing to system faults. Figure S1 shows the baseline data with the interpolated values. In order to avoid possible end effects with the STL decomposition (Pickers and Manning, 2015), the time series were extended by a year both forwards and backwards in time, by taking the interpolated data for the first year and the last year and adding and subtracting the average annual trends for each species (CO_2: 2.31 ppm yr^{-1}, O_2: -24.1 per meg yr^{-1}, APO: -12.0 per meg yr^{-1}). These average annual trends were from an initial run of STL. After the seasonal decompositions were completed, these extended years were removed for all subsequent analyses (including recomputing average annual trends). The baselines, the interpolation of the datasets, and the seasonal decompositions presented here are just one example of the methods and parameters that could be used, since time series decomposition can be susceptible to the choice of method and parameters (Pickers and Manning, 2015).

3 Repeatability and compatibility of the measurement system

The WMO/GAW sets compatibility goals for measurements of greenhouse gas and related species in the atmosphere based on what compatibility is scientifically desirable. Compatibility is a measure of the persistent bias between measurement records (Crotwell et al., 2020). These WMO compatibility goals are ± 0.1 ppm for CO_2 in the Northern Hemisphere and ± 2 per meg for O_2 globally. However, given current analytical capabilities, the O_2 goal is considered somewhat aspirational, as it is not routinely achievable. The WMO also provide an extended compatibility goal of ± 10 per meg for studies where greater accuracy is not required (Crotwell et al., 2020), and which is routinely achievable for some laboratories. Nevertheless, for most applications of O_2 data from our WAO station, the extended compatibility goal is not sufficient, so we strive to get as close to the ± 2 per meg goal as we can. We can also quantify repeatability from our datasets. Repeatability is a measure of the closeness of the agreement between the results of successive measurements over a short period of time (Crotwell et al., 2020). Repeatability goals should be one half of the network compatibility goals, that is, ± 0.05 ppm for CO_2, and ± 1 per meg for O_2 (or ± 5 per meg for the extended O_2 goal). We have several ways in which

to quantify compatibility and repeatability from our WAO datasets, which we discuss in this section, including results from intercomparison programmes, analysing data from our TT, ZT, and WT measurements, and examining the standard deviation of sample air data.

3.1 Intercomparison programmes

WAO has participated in three intercomparison programmes in order to assess the compatibility of WAO with other measurement sites. These intercomparison programmes are: "Cucumbers" (http://www.cucumbers.uea.ac.uk, last access: 17 November 2023); "GOLLUM" (Global Oxygen Laboratories Link Ultra-precise Measurements, http://www.gollum.uea.ac.uk, last access: 17 November 2023); and the WMO/IAEA Round Robin Comparison Experiment (World Meteorological Organization/International Atomic Energy Agency, http://gml.noaa.gov/ccgg/wmorr/index.html, last access: 17 November 2023). These intercomparison programmes involve measuring the same high pressure cylinders filled with dry air, circulated amongst different laboratories and field stations, and comparing the measurements. Each programme includes several trios of cylinders circulating amongst participants, except for the most recent WMO round ("Round 6"), where pairs of cylinders were circulated. The intercomparison results from WAO are shown in Fig. 3 and are plotted as the values measured at WAO minus the values from the first time the cylinders were measured at the central laboratories: Max Planck Institute for Biogeochemistry (MPI-BGC) for the Cucumbers; SIO for the GOLLUMs; and for the WMOs the NOAA/ESRL/GML for CO_2 and the National Center for Atmospheric Research (NCAR), USA. for O_2.

The average offsets at WAO relative to the initial central laboratory analysis, for CO_2 and O_2, are shown in Table 1. The average offset for the GOLLUMs is within the WMO compatibility goal (± 0.1 ppm) but the Cucumbers and WMOs average offsets are larger. The GOLLUMs and Cucumbers $\pm 1\sigma$ standard deviations are slightly larger than ± 0.1 ppm, which implies that the WAO CO_2 measurements are not of sufficiently high precision to have confidence in the average offset. The WMOs $\pm 1\sigma$ standard deviation is less than ± 0.1 ppm, suggesting that the WAO CO_2 measurements are offset from the NOAA CO_2 values, although this is based on only two sets of measurements (in 2010 and 2015). For the Cucumbers, 16 out of the 30 sites involved in the programme, had a $\pm 1\sigma$ standard deviation $> \pm 0.1$ ppm (Manning et al., 2014). This demonstrates that, even for a gas such as CO_2, where measurement precision is routinely achievable to WMO requirements, maintaining such compatibility at field stations over the long-term is still challenging owing to other gas handling and calibration effects, such as leaks, drifting mole fractions within cylinders, and disturbances to the ambient environment, for instance room temperature control issues (Manning et al., 2014).

Table 1. The average offsets at WAO relative to the initial central laboratory analysis for the three intercomparison programmes WAO participated in. These average offsets are the average of the cylinder differences and the $\pm 1\sigma$ standard deviation of the cylinder differences.

Intercomparison programme	CO_2 (ppm)	O_2 (per meg)
GOLLUMs	-0.04 ± 0.11	-0.5 ± 6.0
Cucumbers	-0.11 ± 0.15	5.8 ± 12.3
WMOs	-0.22 ± 0.08	-2.6 ± 2.6

The WMO O_2 average offset is based on only one set of measurements of two cylinders (O_2 analysis was not an option with the WMO programme prior to Round 6). For Cucumbers none of the five sites measuring O_2 were within the ± 2 per meg goal, and four of the five sites were within the ± 10 per meg goal (Manning et al., 2014). The measurements made in 2015 have larger $\pm 1\sigma$ standard deviations, since during this time the WAO O_2 analyser was performing less well (see Sect. 4.1). The GOLLUM cylinders tend to perform better than the Cucumber cylinders for O_2, possibly because Cucumbers was not specifically focused on O_2, and, therefore, the laboratories that were not doing O_2 measurements may not have treated the cylinders in the way that is typically used for O_2 measurements (e.g. vertical storage and non-ideal pressure regulators) and that this could have influenced the O_2 mole fraction in the cylinders. Some of the intercomparison cylinders had O_2 and CO_2 mole fractions outside of the calibration range of our measurement system, which may have influenced the results. The results of the intercomparison programmes should be kept in mind when comparing WAO data to other stations.

3.2 Stability of Target Tank mole fractions

The Target Tank (TT) is used to check the performance of the O_2 and CO_2 measurement system and is typically measured every 11 h. The TT has a dual purpose: firstly, it is used to check how compatible the measurements at WAO are to the UEA CRAM Laboratory, where TT cylinders are usually analysed before being used at WAO. Secondly, the TT can also indicate the repeatability of the WAO CO_2 and O_2 analysers. Between May 2010 and December 2021, 11 TTs were measured at WAO, with a total of 8365 TT measurements, where we define a TT measurement as the mean of seven consecutive 2 min measurements. TT measurements made when there were known technical issues have been removed, resulting in 961 O_2 and 878 CO_2 TT measurements removed, leaving 89 % of the O_2 data and 90 % of the CO_2 data. The TT does not pass through the inlet lines or the first stage of the drying system (Fig. 2), and, therefore, the repeatability of the TT measurements is not a quality control check on the whole measurement system but of the analysers,

the internal calibration, and the gas handling system from the TT to the analysers.

The CO_2 and O_2 TT results as differences from the UEA CRAM Laboratory declared values are shown in Fig. 4, and in Fig. 5, for each TT cylinder, we show the linear trend lines of the TT differences with their slope and Pearson correlation (R^2). Ideally, both the slope of the linear trend line and the R^2 for each cylinder would be zero. Anything other than zero could indicate a drift in the calibration scales defined by the measurement system at WAO or a drift in the mole fractions in the TT itself.

The WAO CO_2 measurements for TT02 and TT07 are both approximately 0.1 ppm lower than the UEA CRAM Laboratory declared values (Fig. 5). For CO_2 TT01 and TT05 both have decreasing trends (Fig. 5); however, these TTs exhibited more variable measurements than the other TTs (Fig. 4), so it is possible that these trends are not robust. All the TTs, except TT01, have linear trend lines with slopes that are less than ± 0.15 ppm yr^{-1} and $R^2 < 0.02$, suggesting that there is no significant drift in CO_2 mole fractions. In September 2012 the TT CO_2 measurements were more variable due to decreased performance of the CO_2 analyser (Fig. 4).

For O_2, there are five cylinders that have a slope greater than ± 2 per meg yr^{-1} (Fig. 5). TT01 has a decreasing trend, and TT05 has an increasing trend; however, these TTs exhibited more variable measurements than the other TTs (Fig. 4), which may have influenced the perceived drifts in their values, and they both have $R^2 < 0.09$. TT01 is a 20 L cylinder (all other TTs are between 40–50 L), and there is evidence that smaller cylinders have less stable mole fractions (Pickers, 2016), and this cylinder was used, with no conditioning, immediately after it had been evacuated. TT05 was the TT being used in 2015 when the Oxzilla precision was poor. TT01 and TT05 are also the cylinders with the poorest compatibility and repeatability, excluding the final cylinder (Table 2). There are three remaining cylinders that show evidence of drift and have $R^2 > 0.09$. TT09 and TT10 both have decreasing O_2 mole fractions during the whole of their run, whereas TT07 O_2 mole fractions only start decreasing during the last 4 months of its run (Fig. 4). For these three cylinders the Zero Tank (ZT) O_2 measurements for the same time periods were investigated (see Sect. 3.3). The ZT is used to adjust the CO_2 calibration c-term, but O_2 is also measured during these runs, because the analysers are connected in series. Therefore, if the ZT O_2 is also drifting then that would indicate that the measurement calibration is drifting, whereas if it is not drifting that would indicate that it is the mole fraction in the TT itself which is drifting. For TT07, TT09, and TT10 the ZT O_2 mole fractions were not drifting at the same time, and, therefore, the drift is most likely caused by the TTs themselves.

Table 2 shows the compatibility of the measurement system which is the average of the differences between the TT measured values and UEA CRAM Laboratory declared values and the $\pm 1\sigma$ standard deviation. The UEA CRAM Lab-
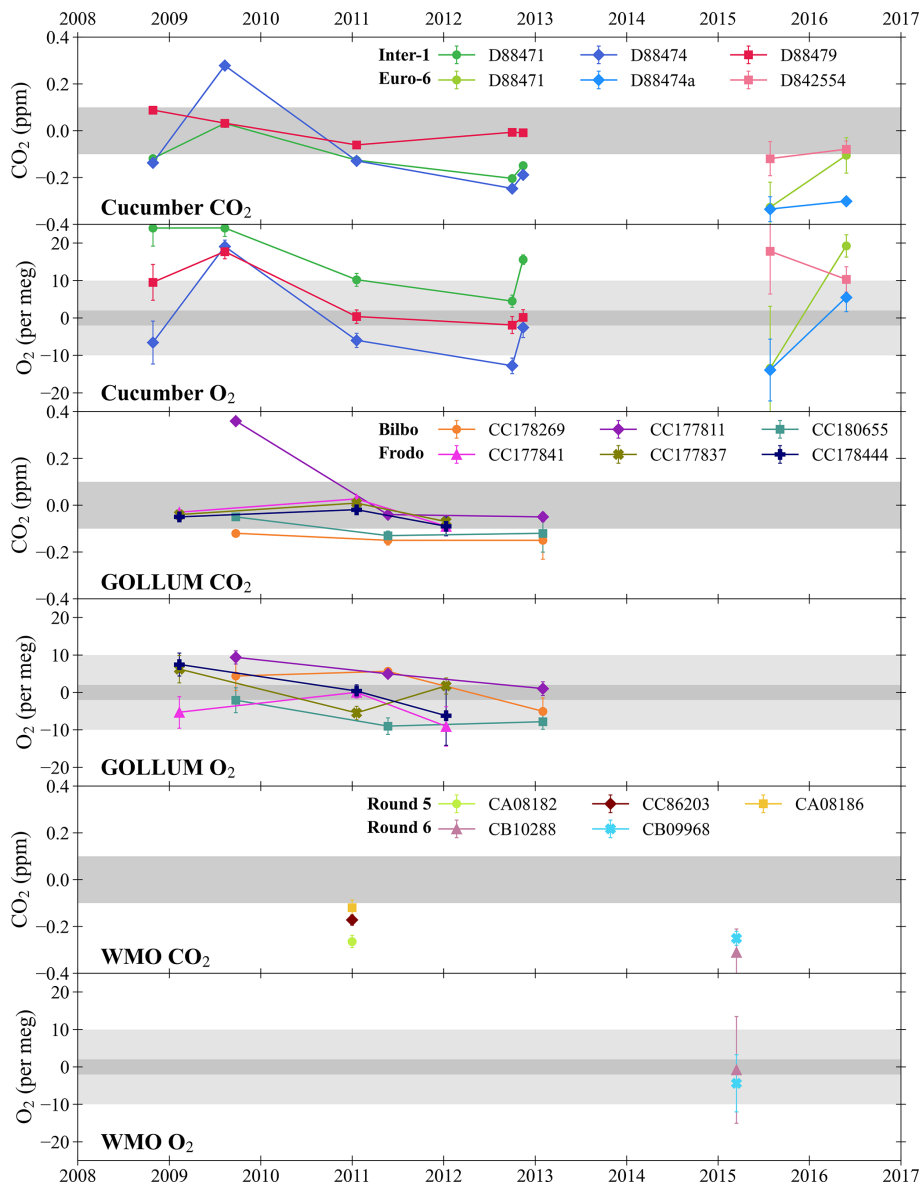
Figure 3. Cucumbers, GOLLUM, and WMO intercomparison cylinder results for CO_2 and O_2 plotted as the WAO measurements minus the initial central laboratory measurements. The horizontal shaded grey bands represent the WMO compatibility goals: ± 0.1 ppm for CO_2, and ± 2 per meg and ± 10 per meg for O_2. The legends state the unique cylinder ID numbers. If the same cylinder was measured more than once throughout the programme, this is indicated by connecting symbols with lines. The error bars show the $\pm 1\sigma$ standard deviation of the cylinder measurements and in some cases the error bars are smaller than the symbols. All programmes involve trios of cylinders, with the exception of "Round 6" of the WMO programme for which there were pairs of cylinders. WAO was originally part of the "Inter-1" Cucumbers rotation but later moved to the "Euro-6" rotation; WAO participated in both the "Frodo" and "Bilbo" GOLLUM rotations concurrently; and WAO participated in "Round 5" and "Round 6" of the WMO Round Robins. The x axis tick marks are at the beginning of each year.

oratory calibration scales are traceable to the WMO CO_2 X2019 scale and the SIO O_2 scale (see Sect. 2.2). The overall compatibility for CO_2 is -0.037 ± 0.146 ppm, which is within the WMO compatibility goal (± 0.1 ppm), although the $\pm 1\sigma$ standard deviation is slightly larger than the compatibility goal. The TT CO_2 compatibility is $< \pm 0.1$ ppm for 67 % of the measurements. The overall compatibility for O_2 is 0.5 ± 4.4 per meg, which is within the compatibility goal

of ± 2 per meg, although the $\pm 1\sigma$ standard deviation is larger than the compatibility goal. The TT O_2 compatibility is $< \pm 2$ per meg for 54 %, $< \pm 5$ per meg for 87 % and $< \pm 10$ per meg for 96 % of the measurements. The average overall compatibility is smaller than the $\pm 1\sigma$ standard deviation for both O_2 and CO_2, meaning that there is not a statistically significant difference between the WAO measurement system and the UEA CRAM Laboratory.
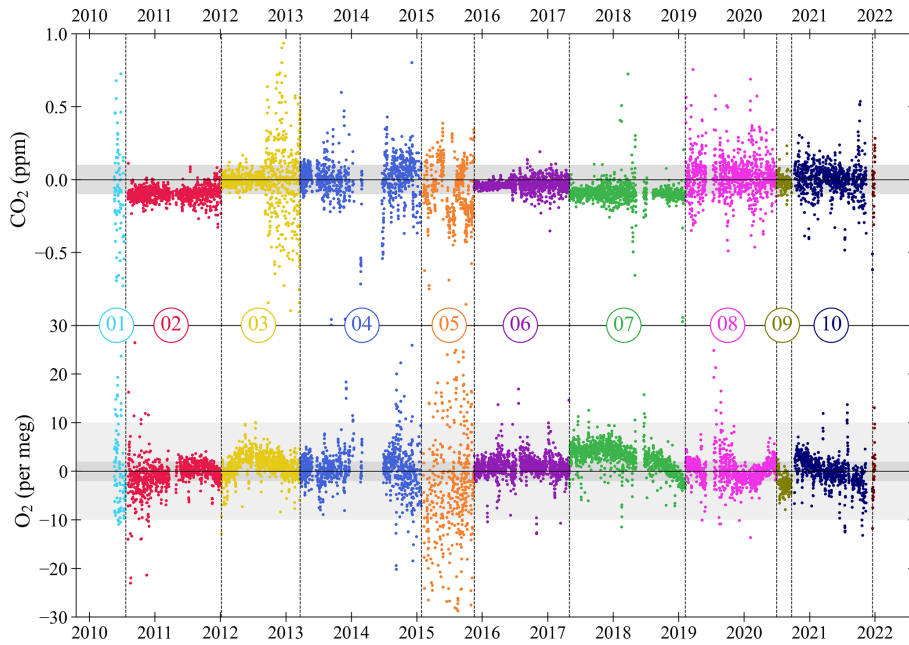
Figure 4. Target Tank (TT) measurements of CO_2 (top panel) and O_2 (bottom panel) at WAO between May 2010 and December 2021. Data are plotted as the difference from the UEA CRAM Laboratory "declared" values (measured minus declared), with each cylinder plotted in a different colour and separated by vertical dashed lines. Cylinders are numbered in the order that they were used. Each TT measurement shown is the mean of seven consecutive 2 min measurements of O_2 and CO_2. Note that 10 and 18 measurements are off scale in the O_2 and CO_2 panels, respectively, out of more than 7000 measurements shown for each species. The O_2 y axis is not visually comparable on a mole per mole basis to the CO_2 y axis. Horizontal black lines are at zero difference, and the horizontal shaded grey bands represent the WMO compatibility goals: ± 0.1 ppm for CO_2, ± 2 per meg and ± 10 per meg for O_2.
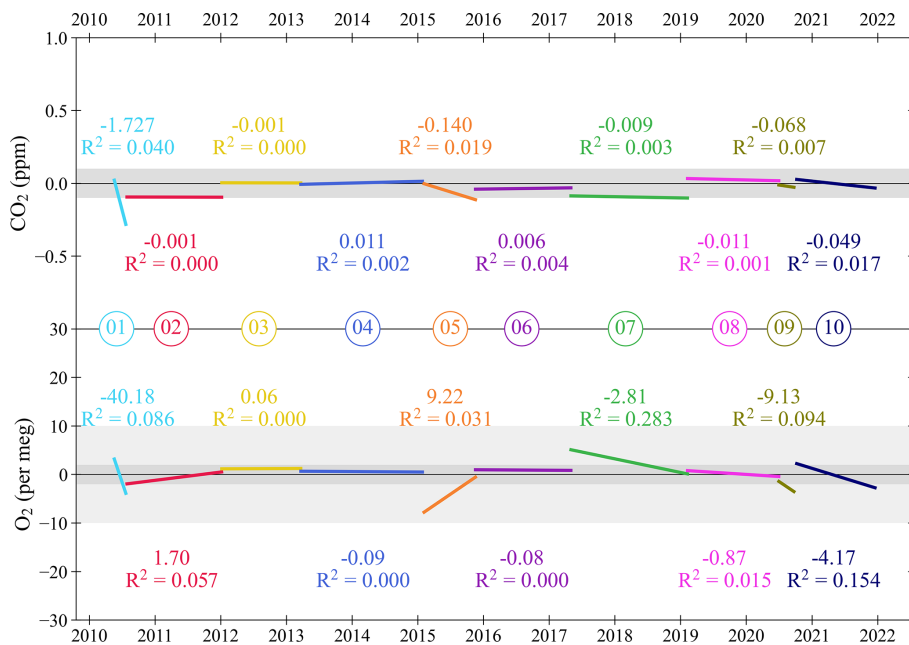

Figure 5. Linear trend lines for each Target Tank (TT), with slopes (in ppm yr^{-1} and per meg yr^{-1}, for CO_2 and O_2, respectively) and R^2 of the Pearson correlation reported for each TT, for CO_2 (top panel) and O_2 (bottom panel) at WAO between May 2010 and December 2021. As in Fig. 4, cylinders are numbered in the order that they were used, horizontal black lines are at zero difference between WAO and UEA, and the horizontal shaded grey bands represent the WMO compatibility goals: ± 0.1 ppm for CO_2, ± 2 per meg and ± 10 per meg for O_2. The 11th TT is not shown as the time period that it was in use is too short for meaningful results.

Table 2. Repeatability and compatibility of the WAO O_2 and CO_2 measurement system indicated by the Target Tanks (TT). Note that we report air measurements between May 2010 and December 2021, so we investigated TT measurements for the same time period; this means the first and last cylinders do not include the whole time period when they were used.

Target Tank	Cylinder ID	Time period	No. of TT runs	Compatibility		Repeatability[b]	
				O_2 (per meg)	CO_2 (ppm)	O_2 (per meg)	CO_2 (ppm)
01	D88528	May 2010–Jul 2010	129	± 7.5[a]	-0.087 ± 0.369	$\pm 5.9 \pm 4.1$	$\pm 0.005 \pm 0.003$
02	D255734	Jul 2010–Jan 2012	1050	-0.7 ± 3.1	-0.095 ± 0.071	$\pm 2.6 \pm 4.3$	$\pm 0.005 \pm 0.003$
03	D743657	Jan 2012–Mar 2013	906	1.2 ± 2.4	0.003 ± 0.216	$\pm 1.7 \pm 1.1$	$\pm 0.004 \pm 0.002$
04	D743656	Mar 2013–Jan 2015	1202	0.6 ± 3.9	0.003 ± 0.151	$\pm 3.3 \pm 5.5$	$\pm 0.005 \pm 0.003$
05	D273555	Feb 2015–Nov 2015	669	-3.6 ± 11.4	-0.065 ± 0.228	$\pm 10.5 \pm 10.6$	$\pm 0.006 \pm 0.003$
06	D801298	Nov 2015–May 2017	1212	0.9 ± 2.3	-0.036 ± 0.040	$\pm 2.3 \pm 2.4$	$\pm 0.003 \pm 0.003$
07	D073406	May 2017–Feb 2019	1259	2.8 ± 2.7	-0.093 ± 0.076	$\pm 2.2 \pm 1.9$	$\pm 0.005 \pm 0.043$
08	D743656	Feb 2019–Jun 2020	982	0.2 ± 3.0	0.025 ± 0.133	$\pm 2.8 \pm 3.7$	$\pm 0.008 \pm 0.043$
09	ND29112	Jun 2020–Sep 2020	152	-2.5 ± 1.8	-0.019 ± 0.050	$\pm 3.0 \pm 1.6$	$\pm 0.004 \pm 0.002$
10	D089506	Oct 2020–Dec 2021	773	± 3.3[a]	± 0.119[a]	$\pm 2.4 \pm 2.4$	$\pm 0.004 \pm 0.002$
11	D258964	Dec 2021–Dec 2021	30	± 5.2[a]	± 0.144[a]	$\pm 9.1 \pm 4.6$	$\pm 0.004 \pm 0.002$
Total		May 2010–Dec 2021	8365	0.5 ± 4.4	-0.037 ± 0.146	$\pm 3.0 \pm 4.6$	$\pm 0.005 \pm 0.023$

[a] These cylinders were not measured at the UEA CRAM Laboratory, so the compatibility cannot be calculated, but the average of the WAO measurements was used to calculate $\pm 1\sigma$ standard deviation for each cylinder. [b] Repeatability was calculated using the same method as Kozlova and Manning (2009) and Pickers et al. (2017), from the mean $\pm 1\sigma$ standard deviations of the average of two consecutive 2 min TT measurements. TT repeatability is reported with $\pm 1\sigma$ uncertainty, which recognises the fact that the measurement system repeatability varies over time.

Table 2 shows the repeatability of the TTs for each cylinder. Each TT data point is the mean of seven consecutive 2 min averages. We calculate the mean of $\pm 1\sigma$ standard deviations for every two consecutive 2 min averages for each TT run. This average of the $\pm 1\sigma$ standard deviation for each TT run is then averaged together for each cylinder and for the whole time period to determine the repeatability. The TT repeatability is reported with the $\pm 1\sigma$ standard deviations of the averages for each TT run. Ideally, the repeatability of a measurement system should be no more than half the compatibility goal, i.e. ± 0.05 ppm for CO_2 and ± 1 per meg/± 5 per meg for O_2.

Overall, the repeatability of the measurement system was $\pm 0.005 \pm 0.023$ ppm for CO_2, which is an order of magnitude smaller than the repeatability goal. For O_2 the overall repeatability was $\pm 3.0 \pm 4.6$ per meg, which is greater than the ± 1 per meg ideal repeatability goal but is within the extended repeatability goal of ± 5 per meg. The CO_2 repeatability is smaller than the CO_2 compatibility, -0.037 ± 0.146 ppm, whereas the O_2 repeatability is larger than the O_2 compatibility, 0.5 ± 4.4 per meg, because O_2 repeatability is much more technically challenging than CO_2 repeatability. The $\pm 1\sigma$ standard deviations for the O_2 repeatability and the O_2 compatibility are similar, ± 4.6 per meg and ± 4.4 per meg, respectively.

3.3 Stability of Zero Tank mole fractions

The Zero Tanks (ZTs) are used to adjust the intercept of the CO_2 calibration curve in-between calibrations to correct for baseline drift in the CO_2 analyser response caused by changes in temperature (see Sect. 2.2). The O_2 in the ZT is

also measured but is not used as part of the calibration. The ZT mole fractions are not measured at the UEA before being sent to WAO, and, therefore, the ZTs cannot be used to assess the compatibility of the WAO system with the UEA CRAM Laboratory. The ZTs can be used to access the O_2 and CO_2 repeatability of the measurement system in the same way as the TTs (see Sect. 3.2).

The ZT is typically measured every 3 to 4 h, and between May 2010 and December 2021 there were 26 359 ZT measurements. Measurements made when the system was experiencing known technical issues have been removed; this was 2672 measurements for CO_2 and 2866 measurements for O_2, leaving 90 % of the CO_2 ZT data and 88 % of the O_2 ZT data. The ZT mole fractions were between 354 ppm and 429 ppm for CO_2. Excluding ZT20, which had an O_2 value of 294 per meg, the ZT O_2 values ranged from -478 per meg to -1363 per meg.

The O_2 and CO_2 ZT mole fractions are shown in Fig. 6 as the difference from the average mole fraction of each cylinder. Table 3 shows the average ZT repeatability calculated in the same way as the TT repeatability (see Sect. 3.2) and the drift in the ZT O_2 mole fractions over time. We can see that there were time periods when the system was more stable and when it was less stable. This, in general, is similar to the TTs; for example, the ZTs also show that 2015 had very noisy oxygen measurements due to poor Oxzilla performance.

ZT03, ZT05, and ZT22 have O_2 mole fractions that drift upwards over time because they were not always stored horizontally (Fig. 6). ZT03 was originally positioned horizontally but then in December 2010 it was moved out of the Blue Box and was positioned vertically, to make space for other cylinders, and this caused the ZT O_2 mole fractions
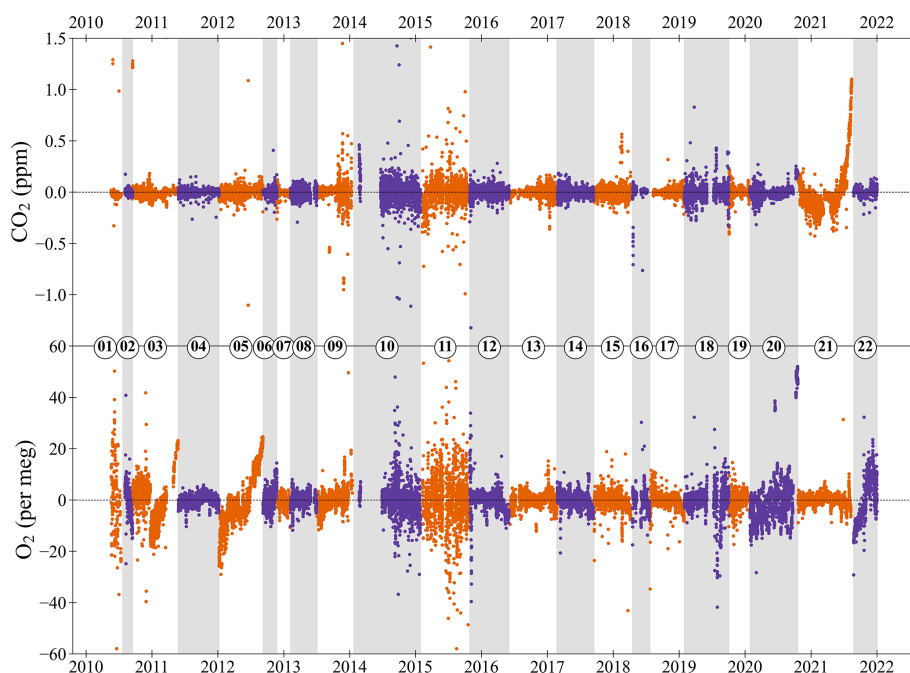
Figure 6. The CO_2 (top panel) and O_2 (bottom panel) Zero Tank (ZT) mole fractions as the difference from the average mole fraction (measurement minus average) for each ZT at WAO between May 2010 and December 2021. The ZTs alternate between orange and purple, and alternate shaded grey bands, to show when the ZT changes. On the y axes "zero" is the average mole fraction for each ZT. The O_2 y axis is not visually comparable on a mole per mole basis to the CO_2 y axis. Cylinders are numbered in the order that they were used. Note that seven and seven measurements are off scale in the O_2 and CO_2 panels, respectively, out of more than 20 000 measurements shown for each species.

to start drifting upwards. ZT05 was positioned vertically for the whole of its run, so its O_2 mole fractions are drifting upwards the whole time. ZT22 was originally positioned vertically and then in November 2021 it was put horizontally, which is why the measurements for ZT22 drift upwards at the beginning and then stop. The ZT O_2 measurement is not used in the calibration, so these drifts do not affect the measurement system performance. ZT02 has O_2 mole fractions that drift downwards over time. The TTs O_2 mole fractions were not drifting at the same time, so it is likely that the ZT itself was drifting, not the measurement system. ZT01 shows a decreasing O_2 linear trend line; however, during this time, the measurements were noisy, so we have low confidence in the slope of the trend.

The CO_2 mole fraction of ZT21 drifts upwards at the end because the internal walls of this cylinder were cleaned using "sand blasting", and it was then measured at WAO to investigate what effect this would have on the stability of the O_2 and CO_2. It was found the CO_2 mole fractions in the cylinder drift upwards at lower pressures, but there was no noticeable effect on O_2. The ZT is used to recalibrate the intercept every 3 to 4 h, and the within-cylinder drift in this time period should be small enough to not affect the measurements. In order to be confident that there is no effect on the measurements, "sandblasted" cylinders should not be used as ZTs once the internal pressure drops below 15 bar.

If we exclude the three ZTs that were vertical, the average CO_2 and O_2 repeatability based on the ZTs is $\pm0.005 \pm 0.019$ ppm and $\pm3.1 \pm 5.3$ per meg, respectively, which is similar to the CO_2 and O_2 repeatability based on the TTs ($\pm0.005 \pm 0.023$ ppm and $\pm3.0 \pm 4.6$ per meg, see Sect. 3.2). These results increase our confidence that this is the repeatability of the measurement system.

Figure 7 shows the absolute difference in the CO_2 mole fractions between the current ZT and the previous ZT (measured 3 to 4 h earlier). The ZT is used to adjust the intercept of the CO_2 calibration curve in-between calibrations, and it is assumed that the difference between the current ZT and the previous ZT is caused by drift in the baseline response of the CO_2 analyser. The average absolute difference in CO_2 is 0.03 ppm, which is less than the ±0.05 ppm repeatability goal, overall, 85 % of the differences are < 0.05 ppm. These differences suggest that the ZT is measured regularly enough that the drift in the baseline is kept small enough to not substantially effect the measurements.

3.4 Stability of calibration coefficients

Three Working Secondary Standard (WSS) cylinders are used to calibrate the measurement system every 47 h (see Sect. 2.2). The c-terms of these equations are discussed in Sect. 3.5. In this section, we discuss the a-term and b-terms

Table 3. Repeatability of the Zero Tank (ZT) O_2 and CO_2 measurements at WAO. We have calculated the O_2 linear trend line for the time period each ZT was used and report here the slope and R^2 of the Pearson correlation. Note that we report air measurements between May 2010 and December 2021, so we investigated ZT measurements for the same time period, this means the first and last cylinders do not include the whole time period when they were used.

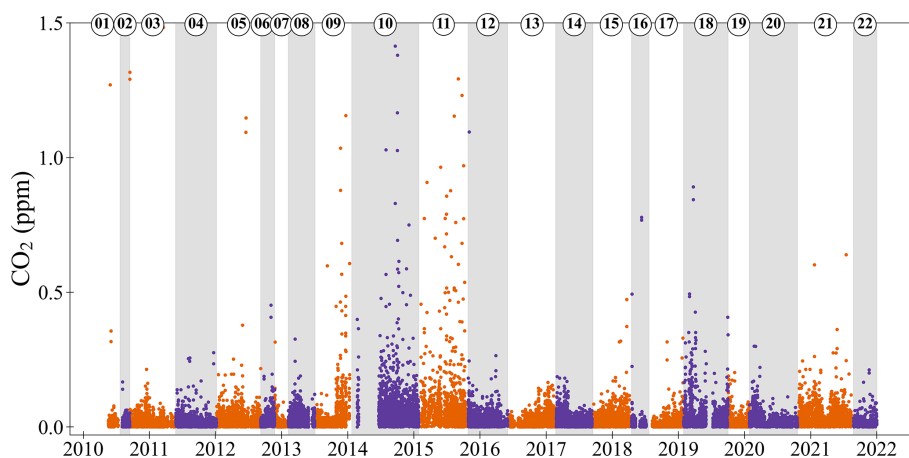| Zero Tank	Time period	No. of ZT runs	O_2 slope (per meg yr^{-1})	O_2 R^2	O_2 repeatability (per meg)	CO_2 repeatability (ppm)
01	May 2010–Jul 2010	220	−127.5	0.099	±7.0 ± 6.7	±0.004 ± 0.002
02	Jul 2010–Sep 2010	306	−150.0	0.373	±5.6 ± 9.5	±0.005 ± 0.003
03	Sep 2010–May 2011	1407	1.3	0.001	±3.7 ± 5.0	±0.006 ± 0.023
04	May 2011–Jan 2012	1276	3.0	0.076	±1.5 ± 0.8	±0.005 ± 0.003
05	Jan 2012–Sep 2012	1323	46.4	0.791	±1.7 ± 0.8	±0.005 ± 0.003
06	Sep 2012–Nov 2012	453	29.8	0.199	±1.8 ± 0.9	±0.003 ± 0.002
07	Nov 2012–Feb 2013	948	−16.2	0.149	±1.8 ± 0.9	±0.003 ± 0.001
08	Feb 2013–Jul 2013	1040	1.2	0.003	±1.8 ± 1.3	±0.004 ± 0.002
09	Jul 2013–Jan 2014	1241	13.3	0.235	±2.3 ± 1.7	±0.006 ± 0.031
10	Jan 2014–Jan 2015	1760	−7.1	0.058	±4.9 ± 8.3	±0.005 ± 0.005
11	Feb 2015–Oct 2015	1903	−0.9	0.000	±10.8 ± 12.3	±0.006 ± 0.003
12	Oct 2015–Jun 2016	1711	−7.7	0.089	±3.4 ± 7.2	±0.003 ± 0.001
13	Jun 2016–Feb 2017	1624	1.1	0.007	±2.2 ± 1.7	±0.004 ± 0.002
14	Feb 2017–Sep 2017	1588	−6.6	0.155	±2.2 ± 1.7	±0.003 ± 0.002
15	Sep 2017–Dec 2017	1555	−5.7	0.086	±2.5 ± 3.2	±0.006 ± 0.029
16	Jun 2018–Jul 2018	636	−10.2	0.047	±2.5 ± 2.8	±0.006 ± 0.054
17	Jul 2018–Jan 2019	1401	−9.2	0.211	±2.0 ± 2.0	±0.003 ± 0.009
18	Jan 2019–Oct 2019	1502	−0.1	0.000	±3.5 ± 5.3	±0.010 ± 0.049
19	Oct 2019–Jan 2020	861	10.6	0.092	±3.0 ± 3.2	±0.004 ± 0.002
20	Jan 2020–Oct 2020	1434	32.9	0.295	±2.2 ± 1.5	±0.003 ± 0.001
21	Oct 2020–Aug 2021	1575	−0.6	0.005	±1.8 ± 1.9	±0.003 ± 0.002
22	Aug 2021–Dec 2021	595	65.8	0.566	±5.7 ± 5.2	±0.004 ± 0.013

Figure 7. Absolute differences between the ZT CO_2 mole fraction and the previous ZT CO_2 mole fraction (current minus previous; typically measured 3 to 4 h earlier). As in Fig. 6, the orange and purple alternating colours, and shaded grey bands, show when the ZT changes, and cylinders are numbered in the order that they were used. Note that 13 measurements are off scale, out of more than 20 000 measurements shown.

of the CO_2 and O_2 calibrations. We also discuss the Pearson correlation coefficient, R^2, of the measured O_2 mole fractions. Each of these parameters is shown in Fig. 8 as a time series. As three WSSs are used, and the CO_2 response is a quadratic equation, the CO_2 R^2 is always exactly 1.0. The

Ultramat and Oxzilla report uncalibrated raw values of CO_2 and O_2 in units of vpm and %, respectively. The calibration coefficient units were converted from ppm vpm^{-1} to ppm for CO_2 and ppmEq %$^{-1}$ to ppmEq for O_2. This conversion was done by multiplying the coefficients by the average analyser
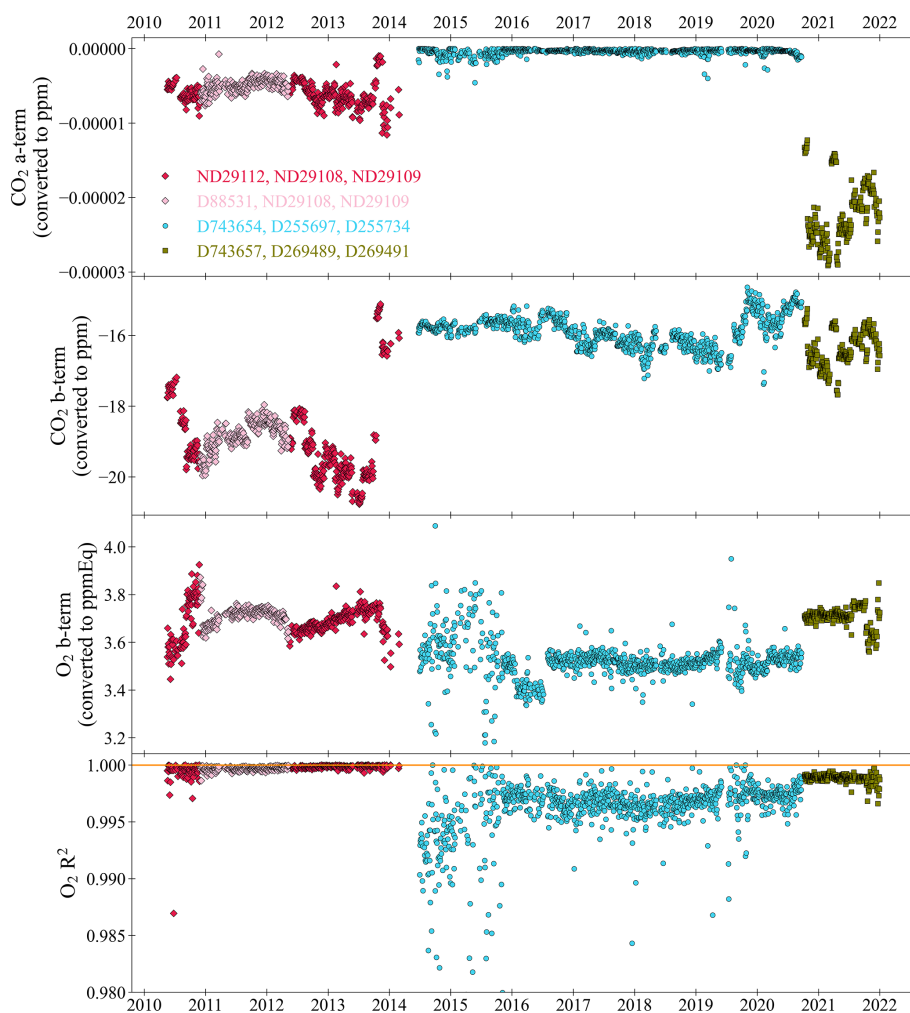
Figure 8. The CO_2 a and b terms, from the CO_2 calibration quadratic equation, $y = ax^2 + bx + c$, and the O_2 b-term and O_2 R^2, from the O_2 calibration linear equation, $y = bx + c$, of the WSS calibrations at WAO between May 2010 and December 2021. The colours and symbols indicate different WSS sets of cylinders and 1.0 on the O_2 R^2 panel is indicated by a horizontal orange line. The c-terms for each species, equivalent to the WT mole fractions, are shown in Fig. 10. Note that five measurements are off scale in the O_2 R^2 panel, out of more than 1700 measurements shown.

response of WSSs between June 2014 and September 2020: D255734 for CO_2 (399.37 ppm, -18.77 vpm) and D743654 for O_2 (-709.0 per meg, -122.7 ppmEq, 0.00072 %). At WAO between May 2010 and December 2021, three sets of WSS cylinders were used (Table 4). In total, there were 2038 calibrations; calibrations when the system was experiencing known technical issues were excluded, this was 277 for CO_2 and 293 for O_2, so this leaves 86 % of the data.

If the calibration coefficient terms drift over time, this could indicate a drift in the analyser sensitivity or a drift in the calibration scale. A drift in the sensitivity of the analyser may impact the precision and the accuracy. By calibrating frequently, the accuracy of the measurement should be less susceptible to drift in the analysers' sensitivity. However, a deterioration in the precision cannot be corrected for. A drift in the calibration scale may be caused by internal drift of

the mole fractions in the calibration cylinders. This can only be determined by reanalysing the calibration cylinders after they have finished being measured at WAO. However, due to practical constraints this is not done on the calibration cylinders used at WAO. While we cannot know if the calibration cylinders have drifted over time, if they had drifted we would expect to see a noticeable step change in the air measurements when the calibration cylinders are changed and/or visible drift in the TT measurements (depending on the rate of the drift). In addition, we would expect to see evidence of long-term drift in our intercomparison programme results.

There are sometimes step changes in the calibration coefficients when the WSS cylinders are changed as the cylinders have different mole fractions in them. There are also sometimes step changes when the cylinders are not changed. These step changes are most likely caused by changes in the

analyser response as it is very unlikely that the mole fractions in the cylinders would suddenly change very quickly and then stop. For example, the CO_2 b-term has a step change in October 2013, when the Ultramat analyser was changed.

The drift in the calibration coefficients was calculated using the slope in the linear trend line for each of the five time periods WSSs were measured for (Table 4). The CO_2 a-term is small, and, therefore, the drift in the CO_2 a-term is also small, less than ± 4 ppt yr^{-1}, indicating that the CO_2 analysers at WAO have a very linear response. There is a large drift between May 2010 and November 2010, the first time ND29112 (Set 1) was used, for both the CO_2 b-term (4.66 ppm yr^{-1}) and O_2 b-term (-3.6 per meg yr^{-1}). The smallest drift in the CO_2 b-term, -0.01 ppm yr^{-1}, occurs between June 2014 and September 2020 when Set 2 of the WSSs is used. For the O_2 b-term, three out of the five periods have drift that is less than ± 0.3 per meg yr^{-1}. The largest drift in the O_2 b-term, 4.1 per meg yr^{-1}, occurs when Set 2 of the WSSs is used, but this is strongly influenced by the calibrations in 2014 and 2015 when there were issues with the measurement system. If the slope is recalculated starting from January 2016 instead, then the drift decreases to -1.9 per meg yr^{-1}. The O_2 and CO_2 mole fractions in the TTs and ZTs were not drifting at the same time (see Sect. 3.2 and 3.3), therefore indicating that it is not the cylinders that are drifting but the analyser sensitivity. The analyser sensitivity drifting should not affect the measurement results so long as the analyser response drift is not significant within a 47 h time period.

The O_2 R_2 varies over time. It is highest and most stable when Set 1 of the WSSs is being measured between 2010 and 2014; on average the O_2 R^2 during this time is 0.9997. In 2014 and 2015, there is additional evidence of the poorer performance of the Oxzilla analyser during this time, and the O_2 R^2 are smaller and much more variable. From 2016 to 2020 the O_2 R^2 is higher and more stable, although it is not as good as it was when Set 1 of the WSSs was being measured, on average the O_2 R^2 during this time is 0.9968. When Set 3 of the WSSs is being measured the O_2 R^2 is higher and more stable than it was with Set 2 but still not as good as it was with Set 1; on average for Set 3 the O_2 R_2 is 0.9988. Overall, from May 2010 to December 2021, the O_2 R^2 is on average 0.9977 and is > 0.995, 92 % of the time.

The calibration range is between the WSS cylinder with the highest mole fraction and the WSS cylinder with the lowest mole fraction. It is intended that the calibration range is large enough to cover the range of mole fractions likely to be measured in the air at WAO. For CO_2, 77 % of the air measurements, 54 out of 73 WTs, 18 out of 22 ZTs, and 7 out of 11 TTs are within the calibration range (Fig. 9). For O_2, 74 % of the air measurements, 31 out of 73 WTs, 9 out of 22 ZTs, and 7 out of 11 TTs, are within the calibration range (Fig. 9). We can have less confidence in the accuracy of mole fractions measured outside the calibration range, and the further away from our calibration range the measurement is, the

less confidence we can have. This is more the case for CO_2, for which the analyser has a non-linear response, than for O_2, which has a linear response.

3.5 Stability of Working Tank mole fractions

Since all measurements are taken against the reference of the Working Tank (WT) this means that the intercept (i.e. the c-term) of the calibration curves for both CO_2 and O_2 is the WT mole fraction at the point of calibration. Calibrations typically take place every 47 h, and the stability of the WT mole fraction over time provides another measure of system performance. Usually, WTs are 50 L cylinders filled to ~ 200 bar, which are used until their pressure gets below ~ 5 bar. The measurement system flow rate is approximately 100 mL min^{-1}, and on average WTs last 55 d. Between May 2010 and December 2021, 76 Working Tanks were measured at WAO. In total there were 2038 calibrations between May 2010 and December 2021. Calibrations made when the system was experiencing known technical issues have been excluded. This leaves 1761 CO_2 calibrations and 1747 O_2 calibrations, or in other words 86 % of the calibrations. WT mole fractions for CO_2 were between 360 and 454 ppm and for O_2 were between -1115 per meg and -362 per meg.

Figure 10 shows the difference between the current WT mole fraction and the average WT mole fraction for each cylinder over its lifetime, as defined by the WSS calibrations. In 2014 and 2015 the WTs mole fractions were much more unstable than they typically are due to multiple technical issues (see Sect. 4.1). The absolute difference of the WT mole fraction between the current calibration and the previous calibration was on average 2.1 ± 3.3 per meg for O_2. This difference is above the WMO repeatability goal of ± 1 per meg, but below the extended repeatability goal of ± 5 per meg. For O_2, the difference between successive calibrations indicates whether the calibration cycle is being run often enough to prevent significant baseline drift. For CO_2, the absolute difference between calibrations is 0.08 ± 0.38 ppm, which is above the repeatability goal of ± 0.05 ppm; however, this does not matter since the WT is redefined every time the ZT is run, so this merely confirms the need to run the ZT every 3 to 4 h in order to correct for CO_2 baseline drift between calibrations.

The O_2 mole fraction decreases as the air in the cylinder is consumed (Figs. 10 and 11). This effect is most likely caused by the preferential desorption of N_2 relative to O_2 from the interior walls of the cylinders as the pressure decreases, owing to the difference in their molecular mass. This effect was previously observed in other studies (Keeling et al., 1998; Manning, 2001; Keeling et al., 2007; Kozlova and Manning, 2009; Wilson, 2012; Pickers, 2016; Barningham, 2018). On average for every 1 bar used O_2 decreases by 0.034 per meg (Fig. 11); assuming a WT starts at 200 bar and finishes at 5 bar, this is a decrease of 6.6 per meg over the lifetime of the

Table 4. All the cylinders that were used as WSSs at WAO. Three sets of WSS cylinders were used (Set 1: May 2010–March 2014, Set 2: June 2014–September 2020, Set 3: October 2020–December 2021). In November 2010, ND29112 was replaced with D88531, then in May 2012 was changed back to ND29112. For each calibration parameter, we report the slope and R^2 of the linear trend line. The slopes of the CO_2 a-terms are in units of $ppt\,yr^{-1}$ (parts per trillion per year). The slopes of the O_2 b-terms were multiplied by 6.05 to convert them from $ppmEq\,yr^{-1}$ to per $meg\,yr^{-1}$.

Set	Cylinder IDs	Start date	End date	CO_2 a-term		CO_2 b-term		O_2 b-term	
				Slope $(ppt\,yr^{-1})$	R^2	Slope $(ppm\,yr^{-1})$	R^2	Slope $(per\,meg\,yr^{-1})$	R^2
1	ND29112 ND29108 ND29109	May 2010	Nov 2010	−3.27	0.29	−4.66	0.82	−3.6	0.68
1	D88531 ND29108 ND29109	Nov 2010	May 2012	0.92	0.19	0.62	0.44	−0.1	0.03
1	ND29112 ND29108 ND29109	May 2012	Mar 2014	−1.09	0.08	0.79	0.07	−0.3	0.20
2	D743654 D255697 D255734	Jun 2014	Sep 2020	0.04	0.02	−0.01	0.00	4.1	0.20
3	D743657 D269489 D269491	Oct 2020	Dec 2021	2.54	0.05	0.42	0.09	−0.2	0.06

cylinder. Previous studies found various depletion amounts: 5 per meg (Keeling et al., 1998), 6 per meg (Manning, 2001), 1 per meg (Keeling et al., 2007), 30 per meg (Kozlova and Manning, 2009), 12 per meg (Wilson, 2012), 54 per meg (Pickers, 2016), 6.6 per meg (Barningham, 2018). Some of these differences can be explained by differences in pressures and flow rates between the different measurement systems (Barningham, 2018) or the use of different types of cylinders (Pickers, 2016). The WT CO_2 does not change as the pressure decreases. The O_2 depletion is not an issue for WTs as their mole fractions are redefined after every WSS calibration (i.e. every 47 h).

3.6 Standard deviation of the air measurements

Figure 12 shows the hourly averages of the $\pm 1\sigma$ standard deviation of the 2 min measurements. For each 2 min measurement there is a $\pm 1\sigma$ standard deviation, which is determined from the 1 min switching of WT and sample air, using 1 s data. These $\pm 1\sigma$ standard deviations for each hour (30 data points if there are no gaps) are then used to calculate the mean. These $\pm 1\sigma$ standard deviations include both the uncertainty in the measurement system and how much the actual CO_2 and O_2 mole fractions in the air vary over a 2 min period. Therefore, these $\pm 1\sigma$ standard deviations cannot be compared to the $\pm 1\sigma$ standard deviations of the Target Tanks or to the repeatability goals.

The $\pm 1\sigma$ standard deviation of the CO_2 measurements is very stable over time (Fig. 12). On average the CO_2 $\pm 1\sigma$ standard deviation is $\pm 0.08 \pm 0.10\,ppm$ and is $< 0.2\,ppm$ 93 % of the time. On average the O_2 $\pm 1\sigma$ standard deviation is $\pm 6.8 \pm 5.4$ per meg and is < 10 per meg, 94 % of the time. In 2014 and 2015 the O_2 $\pm 1\sigma$ standard deviation were much higher and more variable than usual, due to multiple different technical problems in 2014 and poorer performance of the Oxzilla analyser in 2015 (see Sect. 4.1). The 2014 and 2015 O_2 measurements are still accurate, as far as we can tell, but they are not as precise. In general, larger O_2 $\pm 1\sigma$ standard deviations correspond to poorer performance of the Oxzilla analyser.

4 Key features of the WAO atmospheric CO_2, O_2 and APO data

4.1 Time series of CO_2, O_2 and APO

Figure 13 shows a 12-year time series from May 2010 to December 2021 of continuous in situ measurements of CO_2, O_2 and APO at WAO. Measurements continue to the present and are recorded every 2 min. There are gaps in the data caused by cylinder measurements (see Sect. 2.2), changing the WT, routine maintenance, and technical issues. Data collected when the system was experiencing known technical issues have been removed. In total there are 1 930 178 CO_2
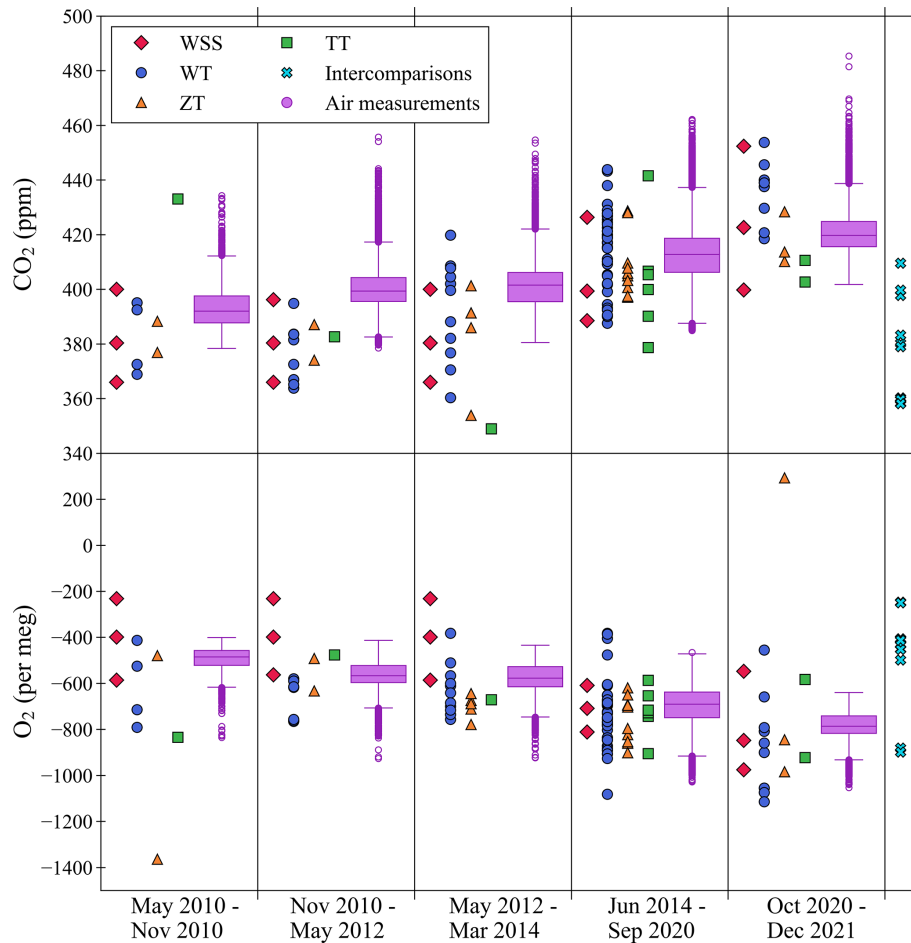
Figure 9. The CO_2 (top panel) and O_2 (bottom panel) mole fractions of the WSSs, WTs, ZTs, TTs, and intercomparison cylinders measured at WAO between May 2010 and December 2021. The air measurements made at WAO during this time are shown as box and whisker plots. The O_2 y axis is not visually comparable on a mole per mole basis to the CO_2 y axis.

measurements and 1 565 908 O_2 measurements (2 min frequency), from 19 May 2010 to 31 December 2021. The data have been averaged to hours to make the dataset more useful for typical applications. Hourly averages are only calculated when there are at least five 2 min measurements in an hour. There are 73 232 CO_2 hourly averages and 69 044 O_2 hourly averages, meaning that there are hourly measurements for 72 % (CO_2) and 68 % (O_2) of the time. Simultaneous measurements of both O_2 and CO_2 are needed to calculate APO.

The proportion of APO data missing in each year varies (Table 5). Measuring the WSSs, TTs, and ZTs takes approximately 14 % of the time in a year, so even if the measurement system ran perfectly, we would still not be able to measure air 100 % of the time. The most complete year was 2017, with only 15 % of the data missing. The year with the most missing data is 2014, where more than half (59 %) of the data are missing; the years 2015, 2018 and 2019 also have a large amount of missing data, 42 %, 46 % and 47 % respectively, due to multiple technical issues. All the other years have between 20 % and 33 % of the data missing (Table 5).

The technical issues in 2014 included: problems with the compressor that opened and closed the pneumatic valves (the on/off, three-way and four-way valves; Fig. 2), the pneumatic valves were replaced with solenoid valves in June 2014; in January and February there was no Ultramat signal because of a broken serial lead, and there was also no ZT; in May 2014 the WSS cylinders were changed; throughout the year there were electrical problems including with the USB hub, data acquisition boards and watchdog board; in June 2014 the red line inlet was blocked with sea salt; there was also a problem with the computer frequently crashing; the PC was replaced in November 2014. The year 2015 has a large amount of missing data, as this year also had technical issues, and a different Oxzilla analyser was used in this year which was not as precise.

The years 2018 and 2019 have a large amount of missing data, because between March 2018 to March 2019 the diaphragm in the KNF pump was torn causing the pump to leak. During this time only one of the inlet lines was being used so this leak affected all the data. Some of these data,
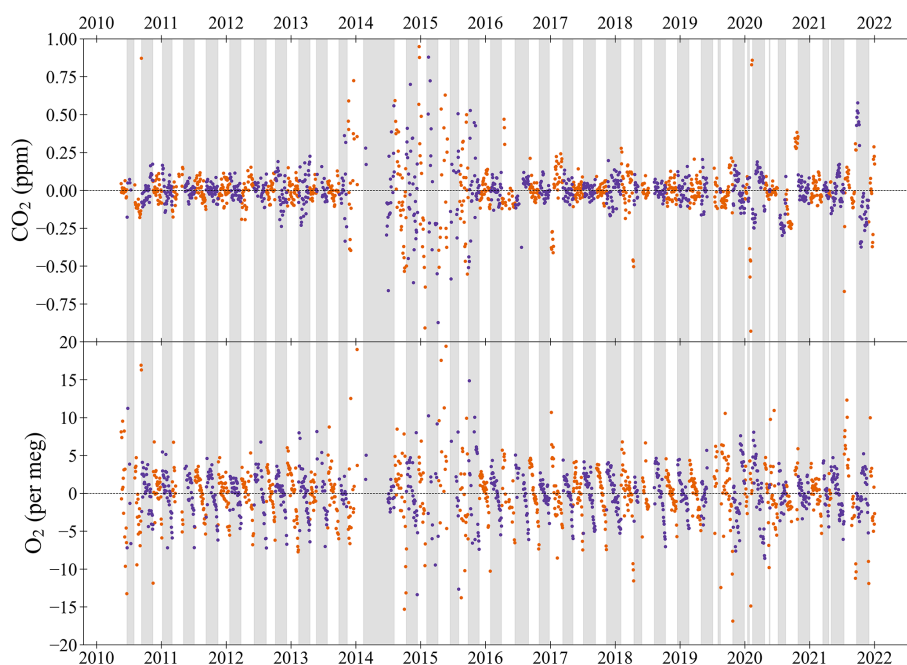
Figure 10. The CO_2 (top panel) and O_2 (bottom panel) Working Tank (WT) mole fractions calculated from the calibrations as the difference from the average mole fraction for each WT (measurement minus average) at WAO between May 2010 and December 2021. The WTs alternate between orange and purple, and alternate shaded grey bands, to show when the WT changes. On the y axes "zero" is the average mole fraction for each WT (dashed line). The O_2 y axis is not visually comparable on a mole per mole basis to the CO_2 y axis. Note that five and seven measurements are off scale in the O_2 and CO_2 panels, respectively, out of more than 1700 measurements shown for each species.

Figure 11. An aggregate of all the O_2 Working Tank (WT) mole fractions determined during all of the calibrations, plotted as the difference from the average mole fraction for each WT (measurement minus average) at WAO between May 2010 and December 2021, plotted versus the WT pressure. The linear trend line is denoted as a dashed black line. Note that five measurements are off scale, out of more than 1700 measurements shown.

Table 5. Annual mean of CO_2, O_2 and APO data at WAO from May 2010 to December 2021. The percentage of APO data missing each year based on the hourly averages is also shown (the APO calculation requires simultaneous CO_2 and O_2 measurements).

Year	CO₂ (ppm)	O₂ (per meg)	APO (per meg)	Missing data (%)
2010	388.11	−477.9	−265.5	30 %
2011	389.88	−494.6	−273.0	30 %
2012	391.97	−516.7	−283.8	23 %
2013	394.44	−536.4	−292.8	33 %
2014	396.74	−554.8	−303.8	59 %
2015	398.85	−579.4	−313.2	42 %
2016	401.53	−609.6	−327.3	29 %
2017	403.98	−636.8	−342.4	15 %
2018	406.30	−666.1	−357.6	46 %
2019	408.80	−688.8	−368.7	47 %
2020	411.57	−709.7	−375.1	20 %
2021	413.86	−731.0	−383.8	24 %

from March 2018 to October 2018, were adjusted using the O_2 measurement record at Cold Bay Alaska, where we were confident of the offset caused by the pump and where we were additionally able to cross-check our correction against an independent dataset from a similar latitude (Shetlands Is-

land, Scotland). However, the size of the leak increased over time, and data from November 2018 to March 2019 could not be adjusted with confidence and were flagged and removed from the quality-controlled dataset. More information on this leaking pump adjustment is provided in supplement.
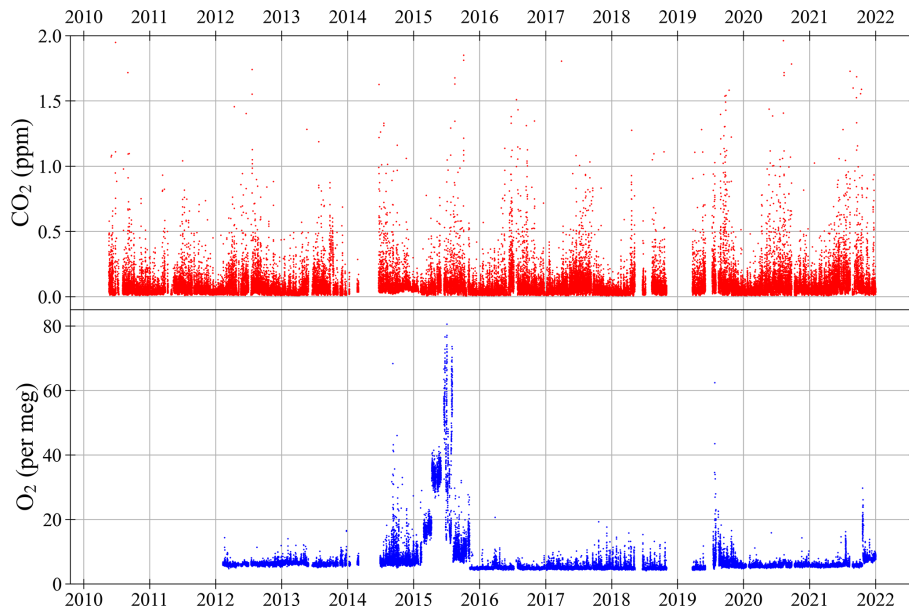
Figure 12. CO_2 (top panel) and O_2 (bottom panel) $\pm 1\sigma$ standard deviation of air measurements at WAO between May 2010 and December 2021. The $\pm 1\sigma$ standard deviations of the 2 min data were not routinely calculated for O_2 until February 2012. Hourly averages of the $\pm 1\sigma$ standard deviations of the 2 min measurements. The O_2 y axis is not visually comparable on a mole per mole basis to the CO_2 y axis. Note that four measurements are off scale in the CO_2 panel, out of more than 70 000 measurements shown.

Figure 13. Hourly averaged CO_2 (top panel), O_2 (middle panel) and APO (bottom panel) at WAO between May 2010 and December 2021. The baselines (yellow lines) are fitted using the RFbaseline function of Ruckstuhl et al. (2012), and the curve fits (black lines) are calculated using the STL function in R (see Sect. 2.3). The O_2 and CO_2 y axes are scaled to be visually comparable on a mole per mole basis. The APO y axis is zoomed in two times, compared to the O_2 y axis on a mole per mole basis. The x axis tick marks are at the beginning of each year.

Table 6. Duration and number of gaps in the dataset, based on APO data.

Duration	No. of gaps	Percent
1 h	2619	9 %
2 h	685	14 %
3 h–1 d	575	26 %
1 d–1 week	98	47 %
1 week–1 month	19	66 %
> 1 month	6	100 %

Most of the gaps in the data only last for short periods of time: 9 % of the missing data are due to gaps lasting 1 h and are usually caused by routine calibrations; 14 % of the missing data are due to gaps lasting 2 h; 26 % of the missing data are due to gaps lasting less than a day; 47 % of the missing data are due to gaps lasting less than a week; and 66 % of the missing data are due to gaps lasting less than a month (Table 6). There are six gaps in the data that last longer than a month. The largest gap in the data is 5 months long, and is it due to the data that had to be removed when the KNF pump was leaking between November 2018 and March 2019. The next longest gap is 4 months long and occurred in 2014 between 2 March and 28 June due to the combination of technical problems described above.

From Fig. 13 we can see there are long-term trends in all three species. On average, atmospheric CO$_2$ at WAO increased by 2.40 ppm yr^{-1} (2.38 to 2.42; 95 % confidence intervals), atmospheric O$_2$ decreased by 24.0 per meg yr^{-1} (24.3 to 23.8), and APO decreased by 11.4 per meg yr^{-1} (11.7 to 11.3). The long-term trends were calculated using the trend from the seasonal decomposition with STL (see Sect. 2.3) and the TheilSen function in the openair package in R (Carslaw and Ropkins, 2012; Carslaw, 2019). These long-term trends are predominantly due to the burning of fossil fuels and land-use changes, which release CO$_2$ and consume O$_2$. Atmospheric O$_2$ is decreasing more quickly than CO$_2$ is increasing because the globally averaged O$_2$: CO$_2$ exchange ratio for fossil fuel combustion is about 1.38 mol mol^{-1} (Keeling and Manning, 2014), and the CO$_2$ increase is buffered by an increasing land carbon sink and ocean carbon sink, whereas the O$_2$ decrease is only buffered by an increasing land oxygen source and a small ocean oxygen source from O$_2$ outgassing (R. F. Keeling et al., 1996).

4.2 Seasonal cycles

The seasonal component of the WAO time series is obtained using the STL decomposition (see Sect. 2.3). The CO$_2$ mole fraction is higher during the Northern Hemisphere winter and lower during the summer due mostly to the terrestrial biosphere (Fig. 14). Vegetation takes in CO$_2$ in the spring and summer in order to grow and releases CO$_2$ in the autumn and winter as it decomposes (Heimann et al., 1989). There is also
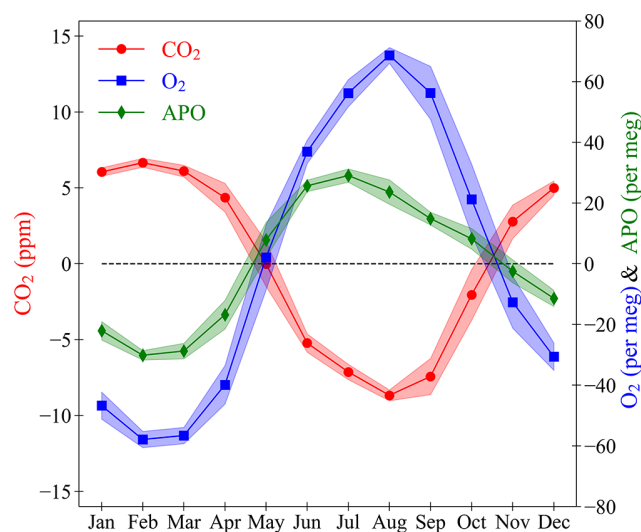

Figure 14. The seasonal cycles of CO$_2$ (red circles, left axis), O$_2$ (blue squares, right axis), and APO (green diamonds, right axis) at WAO. Individual points are the monthly means of the seasonal component of the STL decomposition (see Sect. 2.3). The shaded bands are the average of the $\pm 1\sigma$ standard deviation of the monthly averages of the baseline data. The y axes are scaled to be visually comparable on a mole per mole basis.

an influence from increased temperature and sunlight during the summer leading to increased photosynthesis (Heimann et al., 1989). The exchange of CO$_2$ between the atmosphere and the oceans takes $\sim$ 1 year (Broecker and Peng, 1974), and O$_2$ fluxes from different ocean processes are reinforcing on seasonal timescales, whereas for CO$_2$ these counteract (Keeling and Manning, 2014). The combined effect of the CO$_2$ lag and counteracting CO$_2$ processes is that there is a minimal marine influence on the atmospheric CO$_2$ mole fraction seasonal cycle (Heimann et al., 1989; Randerson et al., 1997).

The O$_2$ mole fraction is lower during the winter and higher during the summer. O$_2$ is anti-correlated with CO$_2$ as they are involved in the same reactions, increased photosynthesis during the spring and summer releases O$_2$ and decomposition during the autumn and winter takes in O$_2$ (Keeling and Shertz, 1992). The air–sea gas exchange of O$_2$ is much quicker than for CO$_2$ and takes $\sim$ 1 month (Broecker and Peng, 1974). During the summer O$_2$ is outgassed from the oceans, and this enhances the O$_2$ seasonal cycle and makes it larger than the CO$_2$ seasonal cycle (Keeling and Shertz, 1992).

APO is lower during the winter and higher during the summer. The seasonal cycle of APO is correlated with the seasonal cycle of O$_2$ and anti-correlated with CO$_2$. APO is invariant to terrestrial biosphere processes. The seasonal cycle of APO is mainly driven by ocean ventilation changes, marine productivity cycling, and the changing solubility of O$_2$ in the oceans as temperature changes (Keeling et al., 1998). There is also a smaller effect on CO$_2$, O$_2$ and APO from

the seasonal cycle of fossil fuel emissions as more fossil fuel combustion takes place during the winter for heating and lighting (Steinbach et al., 2011). There is also a seasonal cycle in the height of the atmospheric boundary layer, that influences all three species (Stephens et al., 2000). The APO seasonal cycle is about half the size of the O_2 cycle ($68/134 = 0.5$) indicating that about half of the O_2 seasonal cycle at WAO is due to terrestrial biosphere processes and about half is due to ocean processes and fossil fuel combustion.

The CO_2 maximum, O_2 minimum and APO minimum occur between January and March each year. The CO_2 minimum and O_2 maximum occur in August or September each year. The APO maximum is more variable and tends to occur earlier in the year between June and August. The peak-to-peak amplitude of the seasonal cycle for CO_2 is 16 ppm (15 to 17 ppm), for O_2 it is 134 per meg (128 per meg to 139 per meg), and for APO it is 68 per meg (62 per meg to 73 per meg). A zero-crossing day is the date at which the detrended curve crosses zero on the y axis (C. D. Keeling et al., 1996). Spring zero crossings occur in April or May each year, and the autumn zero crossings in October or November each year.

4.3   Seasonal variability of diurnal cycles

In general, CO_2 mole fractions are lower during the day and higher at night (Fig. 15). O_2 mole fractions are anti-correlated with CO_2 and are higher during the day and lower at night. APO variations do not exhibit a diurnal cycle at WAO. The diurnal cycles in CO_2 and O_2, like the seasonal cycles, are influenced by changes in the terrestrial biosphere processes of photosynthesis and respiration driven by changes in sunlight and temperature and are influenced by changes in the atmospheric boundary layer height (Stephens et al., 2000; Kozlova et al., 2008). The atmospheric boundary layer is higher during the day and lower during the night, which causes a dilution effect, as molecules during the day are spread out over a larger volume (Denning et al., 1996; Larson and Volkmer, 2008). This amplifies the diurnal cycles in O_2 and CO_2 mole fractions and is referred to as the diurnal rectifier effect. Temperature variations in the oceans that affect gas solubility are not observable on diurnal timescales due to the higher heat capacity of water that can buffer temperature changes.

APO at WAO does not have a diurnal cycle because it is not influenced by the terrestrial biosphere; atmospheric boundary layer effects tend to cancel for APO on diurnal scales, since APO is the sum of two strongly anti-correlated species; and WAO is too remote for APO at the site to be influenced by the diurnal cycle in fossil fuel sources.

There are differences in the diurnal cycles in different seasons. The average amplitude of the diurnal cycles of CO_2 and O_2 are largest in the summer (CO_2: 12.6 ppm, O_2: 60 per meg) and smallest in the winter (CO_2: 3.4 ppm, O_2: 19

per meg). This is due to the combined effect of the diurnal cycle and the seasonal cycle. In the summer, there are higher temperatures, more sunlight and longer days leading to more terrestrial biosphere productivity and larger changes in atmospheric boundary layer height as the differences in temperature between night and day are larger (Bakwin et al., 1995).

In the spring terrestrial productivity is starting to increase, and in the autumn it is starting to decrease as plants die, lose their leaves and become less active. In the winter there are lower temperatures, less sunlight, and shorter days, leading to less activity in the terrestrial biosphere. Also, changes in atmospheric boundary layer height are smaller in the winter as the differences in temperature between the night and day are smaller, so the diurnal rectifier effect is less pronounced (Bakwin et al., 1995). So, the amplitudes of the CO_2 and O_2 diurnal cycles are smallest in the winter.

There are more hours of sunlight during the summer than during the winter, so the summer has a broader peak in O_2 and trough in CO_2 during the day and a shorter peak and trough in the winter. This also effects the timing of the maxima and minima. The CO_2 maximum and O_2 minimum occurs earlier in the summer, at about 04:00, than in the winter, at about 06:00. The CO_2 minimum and O_2 maximum occurs later during the summer at about 17:00 and earlier in winter at about 14:00. Winter CO_2 and O_2 are mostly flat during the night from about 21:00 to 09:00 as the amount of respiration stays mostly the same during the day and the night.

5   Data availability

The accompanying database comprises one csv file. The file contains information on the CO_2, O_2, and APO data (values and associated uncertainties) from Weybourne Atmospheric Observatory.

The file is published by the ICOS Carbon Portal, and is available at https://doi.org/10.18160/Z0GF-MCWH (Adcock et al., 2023).

Other data presented in this paper are available upon request.

6   Conclusions

We have presented a 12-year time series of continuous measurements of CO_2, O_2 and APO at Weybourne Atmospheric Observatory (WAO) in the United Kingdom. The results from the GOLLUM, Cucumbers, and WMO Round Robin intercomparison programmes show that WAO is sometimes but not always within the O_2 and CO_2 WMO compatibility goals established by the high-precision greenhouse gas measurement community. Measurements of Target Tanks indicate that the 2 min O_2 repeatability is $\pm 3.0 \pm 4.6$ per meg, averaged over the 12 years, which is within the extended repeatability goal of ± 5 per meg. Target Tanks CO_2 repeatability is $\pm 0.005 \pm 0.023$ ppm, which is an order of magnitude below
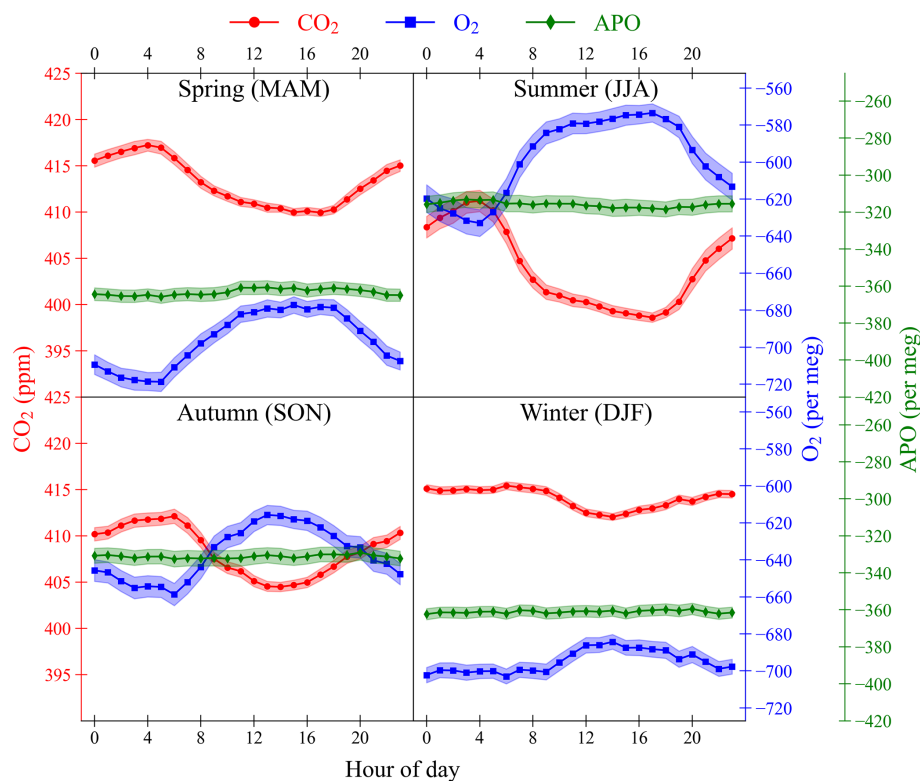
Figure 15. The diurnal cycles of CO_2 (red circles, left axis), O_2 (blue squares, right axis), and APO (green diamonds, right axis) at WAO for each season: spring (MAM), summer (JJA), autumn (SON), and winter (DJF). Individual points are calculated using the 2 min data from May 2010 to December 2021, with the timeVariation function in the OpenAir package in R (Carslaw and Ropkins, 2012). The shaded bands are the average of the $\pm 1\sigma$ standard deviation of the hourly averages of the data. The y axes are scaled to be visually comparable on a mole per mole basis.

the repeatability goal (± 0.05 ppm). Measurements of Zero Tanks indicate that the O_2 repeatability is $\pm 3.1 \pm 5.3$ per meg, and the CO_2 repeatability is $\pm 0.005 \pm 0.019$ ppm, which is similar to the repeatability indicated by the Target Tank measurements. We also show that the calibration coefficients vary over time and the R^2 of the O_2 calibration fit is > 0.995, 92 % of the time. The Working Tanks show that O_2 mole fractions decrease in a cylinder as the pressure decreases. The $\pm 1\sigma$ standard deviations of the air measurements for CO_2 are on average $\pm 0.08 \pm 0.10$ ppm, based on the hourly averages, and are very stable for the whole time series, while the $\pm 1\sigma$ standard deviations for the O_2 air measurements are more variable. Measurements are made every 2 min and between May 2010 and December 2021 there are 1 930 178 CO_2 measurements and 1 565 908 O_2 measurements. There are gaps in the dataset caused by regular calibrations, routine maintenance, and technical issues, and there are six gaps over the 12-year period that last longer than a month. Multiple technical issues in 2014 and 2015 decreased the precision of the data. There are no periods when the Target Tanks, Zero Tanks, and calibration coefficients are all drifting at the same time, indicating that the calibration scale at WAO is likely stable. The time series shows average long-term trends of

2.40 ppm yr^{-1} (2.38 to 2.42) for CO_2, -24.0 per meg yr^{-1} (-24.3 to -23.8) for O_2, and -11.4 per meg yr^{-1} (-11.7 to -11.3) for APO. The average seasonal cycle peak-to-peak amplitude for CO_2 is 16 ppm (15 to 17), for O_2 it is 134 per meg (128 to 139), and for APO it is 68 per meg (62 to 73). The average amplitude of the diurnal cycle in summer is 12.6 ppm for CO_2 and 60 per meg for O_2, and the amplitude of the diurnal cycle in winter is 3.4 ppm for CO_2 and 19 per meg for O_2.

Author contributions. ACM, EAK, AJM, and AJE set up the original measurement system at the Weybourne Atmospheric Observatory. KEA, PAP, ACM, GLF, LSF, TB, PAW, EAK, MH, AJE, and AJM have all been involved in keeping the measurement system running, performing upgrades and improvements, assessing data quality, and carrying out data curation, at various points in time. ACM conceived the design of the system and bespoke software. AJE created and maintains the bespoke software used to run the measurement system. GLF manages the Weybourne Atmospheric

References

Adcock, K., Manning, A., Pickers, P., Forster, G., Fleming, L., Baningham, T., Wilson, P., Kozlova, E., Hewitt, M., Etchells, A., and MacDonald, A.: 12 years of continuous atmospheric O$_2$, CO$_2$ and APO data, Weybourne Atmospheric Observatory, United Kingdom, ICOS Carbon Portal [data set], https://doi.org/10.18160/Z0GF-MCWH, 2023.

Bakwin, P. S., Tans, P. P., Zhao, C., Ussler, W., and Quesnell, E.: Measurements of carbon dioxide on a very tall tower, Tellus B, 47, 535–549, https://doi.org/10.1034/j.1600-0889.47.issue5.2.x, 1995.

Barningham, T.: Detection and Attribution of Carbon Cycle Processes from Atmospheric O$_2$ and CO$_2$ Measurements at Halley Research Station, Antarctica and Weybourne Atmospheric Observatory, U.K., University of East Anglia, https://cramlab.uea.ac.uk/Publications.php (last access: 17 November 2023), 2018.

Blaine, T. W., Keeling, R. F., and Paplawsky, W. J.: An improved inlet for precisely measuring the atmospheric Ar/N$_2$ ratio, Atmos. Chem. Phys., 6, 1181–1184, https://doi.org/10.5194/acp-6-1181-2006, 2006.

Broecker, W. S. and Peng, T.-H.: Gas exchange rates between air and sea, Tellus, 26, 21–35, https://doi.org/10.1111/j.2153-3490.1974.tb01948.x, 1974.

Carslaw, D. C.: The openair manual – open-source tools for analysing air pollution data, Manual for version 2.6-6, University of York, https://davidcarslaw.com/project/openair/ (last access: 17 November 2023), 2019.

Carslaw, D. C. and Ropkins, K.: Openair – An r package for air quality data analysis, Environ. Model. Softw., 27–28, 52–61, https://doi.org/10.1016/j.envsoft.2011.09.008, 2012.

Chevallier, F. and the WP4 CHE partners.: CO$_2$ Human Emissions (CHE) Project: D4.4 Sampling strategy for additional tracers, https://www.che-project.eu/node/243 (last access: 17 November 2023), 2021.

Cleveland, R. B., Cleveland, W. S., McRae, J. E., and Terpenning, I.: STL: A seasonal-trend decomposition procedure based on Loess, J. Off. Stat., 6, 3–73, 1990.

Crotwell, A., Lee, H., and Steinbacher, M. (Eds.): 20th WMO/IAEA Meeting on Carbon Dioxide, Other Greenhouse Gases and Related Measurement Techniques (GGMT-2019), Global Atmosphere Watch (GAW) Report No. 255, Jeju Island, South Korea, https://library.wmo.int/doc_num.php?explnum_id=10353 (last access: 17 November 2023), 2020.

Denning, A. S., Randall, D. A., Collatz, G. J., and Sellers, P. J.: Simulations of terrestrial carbon metabolism and atmospheric CO$_2$ in a general circulation model. Part 2: Simulated CO$_2$ concentrations, Tellus B, 48, 543–567, https://doi.org/10.3402/tellusb.v48i4.15931, 1996.

Hall, B. D., Crotwell, A. M., Kitzis, D. R., Mefford, T., Miller, B. R., Schibig, M. F., and Tans, P. P.: Revision of the World Meteorological Organization Global Atmosphere Watch (WMO/GAW) CO$_2$ calibration scale, Atmos. Meas. Tech., 14, 3015–3032, https://doi.org/10.5194/amt-14-3015-2021, 2021.

Heimann, M., Keeling, C. D., and Tucker, C. J.: A three dimensional model of atmospheric CO$_2$ transport based on observed winds: 3. Seasonal cycle and synoptic time scale variations, in: Aspects of Climate Variability in the Pacific and the Western Americas, Geophys. Monogr. Ser., 55, 277–303, https://doi.org/10.1029/GM055p0277, 1989.

Ishidoya, S., Tsuboi, K., Niwa, Y., Matsueda, H., Murayama, S., Ishijima, K., and Saito, K.: Spatiotemporal variations of the δ(O$_2$/N$_2$), CO$_2$ and δ(APO) in the troposphere over the western North Pacific, Atmos. Chem. Phys., 22, 6953–6970, https://doi.org/10.5194/acp-22-6953-2022, 2022.

Keeling, C. D., Chin, J. F. S., and Whorf, T. P.: Increased activity of northern vegetation inferred from atmospheric CO$_2$ measurements, Nature, 382, 146–149, https://doi.org/10.1038/382146a0, 1996.

Keeling, R. and Shertz, S.: Seasonal and interannual variations in atmospheric oxygen and implications for the global carbon cycle, Nature, 358, 723–727, https://doi.org/10.1038/358723a0, 1992.

Keeling, R. F. and Manning, A. C.: Studies of Recent Changes in Atmospheric O$_2$ Content, 2nd ed., Elsevier Ltd., 385–404 pp., https://doi.org/10.1016/B978-0-08-095975-7.00420-4, 2014.

Keeling, R. F., Najjar, R. P., Bender, M. L., and Tans, P. P.: What atmospheric oxygen measurements can tell us about the global carbon cycle, Global Biogeochem. Cycles, 7, 37–67, https://doi.org/10.1029/92gb02733, 1993.

Keeling, R. F., Piper, S. C., and Heimann, M.: Global and hemispheric CO$_2$ sinks deduced from changes in atmospheric O$_2$ concentration, Nature, 381, 218–221, https://doi.org/10.1038/381218a0, 1996.

Keeling, R. F., Stephens, B. B., Najjar, R. G., Doney, S. C., Archer, D., and Heimann, M.: Seasonal variations in the atmospheric O$_2$/N$_2$ ratio in relation to the kinetics of air-sea gas exchange, Global Biogeochem. Cycles, 12, 141–163, https://doi.org/10.1029/97GB02339, 1998.

Keeling, R. F., Manning, A. C., Paplawsky, W. J., and Cox, A. C.: On the long-term stability of reference gases for atmospheric O$_2$/N$_2$ and CO$_2$ measurements, Tellus B, 59, 3–14, https://doi.org/10.1111/j.1600-0889.2006.00196.x, 2007.

Keeling, R. F., Walker, S. J., and Paplawsky, W.: Span Sensitivity of Scripps Interferometric Oxygen Analyzer. UC San Diego: Scripps Institution of Oceanography, https://escholarship.org/uc/item/7tt993fj (last access: 17 November 2023), 2020.

Kozlova, E. A. and Manning, A. C.: Methodology and calibration for continuous measurements of biogeochemical trace gas and O$_2$ concentrations from a 300-m tall tower in central Siberia, Atmos. Meas. Tech., 2, 205–220, https://doi.org/10.5194/amt-2-205-2009, 2009.

Kozlova, E. A., Manning, A. C., Kisilyakhov, Y., Seifert, T., and Heimann, M.: Seasonal, synoptic, and diurnal-scale variability of biogeochemical trace gases and O$_2$ from a 300-m tall tower in central Siberia, Global Biogeochem. Cycles, 22, 1–16, https://doi.org/10.1029/2008GB003209, 2008.

Larson, V. E. and Volkmer, H.: An idealized model of the one-dimensional carbon dioxide rectifier effect, Tellus B, 60, 525–536, https://doi.org/10.1111/j.1600-0889.2008.00368.x, 2008.

Machta, L. and Hughes, E.: Atmospheric Oxygen in 1967 to 1970, Science, 168, 1582–1584, https://doi.org/10.1126/science.168.3939.1582, 1970.

Manning, A. C.: Temporal variability of atmospheric oxygen from both continuous measurements and a flask sampling network: Tools for studying the global carbon cycle, PhD thesis, University of California, https://cramlab.uea.ac.uk/Publications.php (last access: 17 November 2023), 2001.

Manning, A. C. and Keeling, R. F.: Global oceanic and land biotic carbon sinks from the Scripps atmospheric oxygen flask sampling network, Tellus B, 58, 95–116, https://doi.org/10.1111/j.1600-0889.2006.00175.x, 2006.

Manning, A. C., Schmidt, M., Jordan, A., Levin, I., Hewitt, M., Etchells, A., Pickers, P. A., Hammer, S., Delmotte, M., Vermeulen, A., Alemanno, M., Allison, C., Apadula, F., Arduini, J., Barcza, Z., Brand, W., Chen, H., Ernst, M., Hall, B. D., Haszpra, L., Hatakka, J., Huang, L., Katsumata, K., Kazan, V., Keronen, P., Langenfelds, R., Lavric, J., Leuenberger, M. C., Lopez, M., Machida, T., Meinhardt, F., Moncrieff, J., Necki, J., O'Doherty, S., Piacentino, S., Richter, J., Ries, L., Rothe, M., Scheeren, H. A., Schibig, M. F., Steele, L. P., Szilagyi, I., Wastine, B., Wilson, P. A., Worthy, D. E., and Yver, C.: Integrated non-CO$_2$ Observing System (InGOS) "Cucumbers" intercomparison report, Compatibility of atmospheric greenhouse gas measurements in the InGOS network as assessed by the "Cucumbers" intercomparison programme, https://cucumbers.uea.ac.uk/documents/2014_InGOS_NA3_Cucumbers_Report.pdf (last access: 17 November 2023), 2014.

Nevison, C. D., Munro, D. R., Lovenduski, N. S., Keeling, R. F., Manizza, M., Morgan, E. J., and Rodenbeck, C.: Southern Annular Mode Influence on Wintertime Ventilation of the Southern Ocean Detected in Atmospheric O$_2$ and CO$_2$ Measurements, Geophys. Res. Lett., 47, e2019GL085667, https://doi.org/10.1029/2019gl085667, 2020.

Patecki, M. and Manning, A. C.: First results from shipboard atmospheric O$_2$ and CO$_2$ measurements over the North Atlantic Ocean, Oceans, 2007, 1–6, https://doi.org/10.1109/OCEANSE.2007.4302351, 2007.

Pickers, P. A.: New applications of continuous atmospheric O$_2$ measurements: meridional transects across the Atlantic Ocean, and improved quantification of fossil fuel-derived CO$_2$, PhD thesis, University of East Anglia, https://cramlab.uea.ac.uk/Publications.php (last access: 17 November 2023), 2016.

Pickers, P. A. and Manning, A. C.: Investigating bias in the application of curve fitting programs to atmospheric time series, Atmos. Meas. Tech., 8, 1469–1489, https://doi.org/10.5194/amt-8-1469-2015, 2015.

Pickers, P. A., Manning, A. C., Sturges, W. T., Le Quéré, C., Mikaloff Fletcher, S. E., Wilson, P. A., and Etchells, A. J.: In situ measurements of atmospheric O$_2$ and CO$_2$ reveal an unexpected O$_2$ signal over the tropical Atlantic Ocean, Global Biogeochem. Cycles, 31, 1289–1305, https://doi.org/10.1002/2017GB005631, 2017.

Pickers, P. A., Manning, A. C., Quéré, C. Le, Forster, G. L., Luijkx, I. T., Gerbig, C., Fleming, L. S., and Sturges, W. T.: Novel quantification of regional fossil fuel CO$_2$ reductions during COVID-19 lockdowns using atmospheric oxygen measurements, Sci. Adv., 8, eabl9250, https://doi.org/10.1126/sciadv.abl9250, 2022.

Randerson, J. T., Thompson, M. V., Conway, T. J., Fung, I. Y., and Field, C. B.: The contribution of terrestrial sources and sinks to trends in the seasonal cycle of atmospheric carbon dioxide, Global Biogeochem. Cycles, 11, 535–560, https://doi.org/10.1029/97GB02268, 1997.

Resplandy, L., Keeling, R. F., Eddebbar, Y., Brooks, M., Wang, R., Bopp, L., Long, M. C., Dunne, J. P., Koeve, W., and Oschlies, A.: Quantification of ocean heat uptake from changes in atmospheric O$_2$ and CO$_2$ composition, Sci. Rep., 9, 20244, https://doi.org/10.1038/s41598-019-56490-z, 2019.

Ruckstuhl, A. F., Henne, S., Reimann, S., Steinbacher, M., Vollmer, M. K., O'Doherty, S., Buchmann, B., and Hueglin, C.: Robust extraction of baseline signal of atmospheric trace species using local regression, Atmos. Meas. Tech., 5, 2613–2624, https://doi.org/10.5194/amt-5-2613-2012, 2012.

Ruckstuhl, A. F., Unternaehrer, T., and Locher, R.: IDPmisc: Utilities of Institute of Data Analyses and Process Design, R package version 1.1.20, https://CRAN.R-project.org/package=IDPmisc (last access: 9 March 2023), 2020.

Severinghaus, J. P.: Studies of the Terrestrial O_2 and Carbon Cycles in Sand Dune Gases and in Biosphere 2, PhD thesis, Columbia University, https://doi.org/10.2172/477735, 1995.

Steinbach, J., Gerbig, C., Rödenbeck, C., Karstens, U., Minejima, C., and Mukai, H.: The CO_2 release and Oxygen uptake from Fossil Fuel Emission Estimate (COFFEE) dataset: effects from varying oxidative ratios, Atmos. Chem. Phys., 11, 6855–6870, https://doi.org/10.5194/acp-11-6855-2011, 2011.

Stephens, B. B., Keeling, R. F., Heimann, M., Six, K. D., Murnane, R., and Caldeira, K.: Testing global ocean carbon cycle models using measurements of atmospheric O_2 and CO_2 concentration, Global Biogeochem. Cycles, 12, 213–230, https://doi.org/10.1029/97GB03500, 1998.

Stephens, B. B., Wofsy, S. C., Keeling, R. F., Tans, P. P., and Potosnak, M. J.: The CO_2 budget and rectification airborne study: Strategies for measuring rectifiers and regional fluxes, Inverse Methods in Global Biogeochem. Cycles Geophys. Monogr., 114, 311–324, https://doi.org/10.1029/GM114p0311, 2000.

Stephens, B. B., Keeling, R. F., and Paplawsky, W. J.: Shipboard measurements of atmospheric oxygen using a vacuum-ultraviolet absorption technique, Tellus B, 55, 857, https://doi.org/10.3402/tellusb.v55i4.16386, 2003.

Stephens, B. B., Bakwin, P. S., Tans, P. P., Teclaw, R. M., and Baumann, D. D.: Application of a differential fuel-cell analyzer for measuring atmospheric oxygen variations, J. Atmos. Ocean. Tech., 24, 82–94, https://doi.org/10.1175/JTECH1959.1, 2007.

Thompson, R. L., Manning, A. C., Lowe, D. C., and Weatherburn, D. C.: A ship-based methodology for high precision atmospheric oxygen measurements and its application in the Southern Ocean region, Tellus B, 59, 643–653, https://doi.org/10.1111/j.1600-0889.2007.00292.x, 2007.

Tohjima, Y., Terao, Y., Mukai, H., Machida, T., Nojiri, Y., and Maksyutov, S.: ENSO-related variability in latitudinal distribution of annual mean atmospheric potential oxygen (APO) in the equatorial Western Pacific, Tellus B, 67, 25869, https://doi.org/10.3402/tellusb.v67.25869, 2015.

Wilson, P.: Insight into the Carbon Cycle from Continuous Measurements of Oxygen and Carbon Dioxide at Weybourne Atmospheric Observatory, UK, PhD thesis, University of East Anglia, https://cramlab.uea.ac.uk/Publications.php (last access: 17 November 2023), 2012.